# Design of broadband propagators in two-level systems

G. Goelman, S. Vega, and D. B. Zax
*Department of Isotope Research, Weizmann Institute of Science, Rehovot 76100, Israel*
(Received 28 October 1988)

We describe a method suitable for the design of broadband propagators in two-level or pseudo-two-level systems via amplitude-modulated irradiation. Irradiation sequences are described in terms of a Fourier expansion. The Fourier coefficients of the expansion are used to calculate the time-independent Floquet Hamiltonian which represents the time-dependent Hamiltonian. This transformation removes the difficulty of integrating the time-dependent equations of motion. The infinite Floquet matrix is approximately diagonalized by an application of perturbation theory. A set of infinite matrix operators is introduced which assists in the diagonalization. The perturbation-theory expressions are used to derive approximate expressions for the propagator. Successive terms in the perturbation expansion can be nulled by considering additional Fourier coefficients. Broadband-irradiation sequences with low mean power or low peak power are described corresponding to coherent excitation in two-level systems through the flip angles 45°, 90°, 135°, and 180°.

## I. INTRODUCTION

In this paper we present a general technique for the design of arbitrary broadband propagators in two-level systems with amplitude-modulated pulses. By broadband it is implied that over some range of offset values from the resonance condition the propagator behaves (to within some specified, if necessarily arbitrary, criterion) independently of offset. The excitation sequences we describe are of finite extent in time and constructed, because of their theoretical derivation, by adding together an on-resonance irradiation field (which guarantees that for offset values of zero the two-level system undergoes the desired evolution) with a series of sinusoidal modulation sidebands. Thus the irradiation schemes correspond to a very special set of amplitude-modulated pulses. The heart of the theoretical problem which we address in this paper is how to efficiently analyze the effect of a time-dependent irradiation sequence so as to be able to make predictions about which modulation schemes will be interesting or effective.

Our motivation in this work, and the inspiration for our efforts, has been the introduction in recent years of a variety of composite pulse sequences for use in nuclear magnetic resonance (NMR).[1,2] Such composite pulses have been suggested and implemented for a number of special cases; in particular, for use either where broadband excitation is desired (i.e., where the propagator is independent of resonance offset)[3,4] or in situations where narrow-band excitation is required[5–7] (i.e., where the propagator is designed so that its dependence on offset near the resonance condition is strong). These pulses are, of course, only special cases of the more general and difficult case of describing a desired response and then designing the pulse sequence which will result in that response curve. No general solution is known to the latter problem.

Most of the previous work is derived from the field of NMR, which is also our field of specialization. The theoretical background most often assumes that the system can be described by a pair of interacting energy levels only, and therefore all of the results are largely transportable to coherent optical spectroscopy even if our treatment is presented in the language more familiar to magnetic resonance.[8] In addition, while the vast majority of composite pulses have been designed for the important case of 180° pulses, which are particularly useful for population inversion and in heteronuclear decoupling,[9,10] in the work we present in this paper such pulses are derived as only a special case of a much more general theoretical presentation. To the best of our knowledge, there exists only one other similarly general treatment in the literature.[11] Furthermore, because of the relative underdevelopment of efficient theoretical methods for the calculation of the effect of continuously time-dependent fields, there are relatively few composite pulses designed where the intensity as well as phase of the irradiation are allowed to vary with time.[5,6,12,13] Nonetheless, the potential of amplitude-modulated pulses has been amply demonstrated even though only a small number of such pulse sequences have been introduced. Our expectation is that because constant-amplitude pulses are only a special case of the time-dependent pulses we discuss in this paper, the methods we present here should prove more efficient; i.e., provide equivalent excitation behavior with a smaller investment of irradiation power. We have previously presented some of the preliminary results of this investigation elsewhere.[14]

### A. Background from nuclear magnetic resonance

For both theoretical and technical reasons, most pulses discussed in the literature and implemented in the laboratory are of constant intensity and vary only in phase. Nonetheless, even those few compensated pulses which exploit the additional parameter of amplitude modulation

 

have been demonstrated to be very powerful, and many are routinely implemented in magnetic resonance imaging[13] (MRI), where optimum performance is directly related to commercial profitability.

The realization that a sequential application of a set of rf pulses can generate responses inaccessible from simple strong or weak irradiation is not new. The idea of selective and narrow-band excitation, for example, is already more than ten years old. Redfield, Kunz, and Ralph[15] developed pulse sequences which allow for presaturation of the solvent line which may interfere with the interpretation of high-resolution NMR spectra. More recently these ideas were extended by Hore[16] and by Turner,[17] who developed new narrow-band solvent-suppression pulse cycles, and by Morris and Freeman's DANTE cycle.[18]

Broadband sequences, and in particular broadband spin-inversion pulse sequences, have also found wide applicability because of their relevance to the important problem of efficient heteronuclear decoupling in high-resolution NMR.[9,10] Levitt and Freeman designed the first very important composite $\pi$ pulses used in decoupling schemes, which provide compensation for the undesirable effects of off-resonance irradiation and rf inhomogeneity.[19] Further developments in decoupling schemes based on the theoretical approach introduced by Waugh led to the very efficient WALTZ sequences derived by Shaka, Keeler, Frenkiel, and Freeman.[20]

The demand for compensated pulse sequences is not limited to the problems of solvent suppression or decoupling; interest in such schemes is far more general. Thus, in parallel to developments in decoupling schemes, a variety of composite pulses have been presented which provide compensation for finite flip angles other than 180°.[21–24] (By finite we imply also that the pulse is limited in extent in time and requires only finite-irradiation fields.)

The subset of compensated pulse sequences where amplitude modulation is also exploited is significantly more limited. Amplitude- and phase-modulated excitation pulses based on principles related to self-induced transparency were demonstrated to invert spin-magnetization vectors over a range of off-resonance values.[5,25,26] Slice-selective narrow-band pulses for spatial localization in MRI are routinely amplitude modulated.[13] The Hermite pulses introduced by Warren have been used for accurate narrow-band inversion of inhomogeneously broadened lines.[6]

Almost all composite pulse sequences are developed based on some theoretical approach to the correction of imperfections in or undesirable aspects of normal pulse performance. Some sources of imperfections are inherent; no technical improvements can guarantee irradiation on resonance at several frequencies simultaneously in samples characterized by a range of chemical shifts. Compensation for inevitable imperfections of whatever source can be at least partially achieved by combining small pulse units intelligently so that errors tend to cancel rather than propagate. The fundamental difficulty in designing compensated sequences is that, because almost all interesting experiments are performed using pulses equal to or greater than 90°, linear-response theory cannot reliably be applied. Furthermore, because of the noncommutativity of rotations about several directions, native intuition tends to be misleading. Therefore, in most cases of broadband excitation, average Hamiltonian theory[27] has been applied both to uncover the basic building blocks of composite pulses, and to achieve proper compensation for undesired effects. (Notable exceptions to this statement are Waugh's exact theory of decoupling,[9] sequences derived from self-induced transparency,[28] where the irradiation sequence is given as an exact solution to the Bloch differential equations,[5,25,26] and to the slice-selective MRI sequences where the approach appears to be entirely a numerical optimization.[13])

Application of average Hamiltonian theory (AHT) requires the evaluation of successive terms in the Magnus expansion.[29] For sequences where the field amplitude is fixed and only the phase varies in time, AHT seems a convenient if often times tedious method for calculating the effective Hamiltonian which describes the evolution of the spin system. However, we have found that this analysis scheme may prove cumbersome when amplitude-modulated irradiation fields are introduced into the Hamiltonian. That most of the other schemes which utilize or analyze the impact of amplitude-modulated fields are derived without reference to AHT seems to confirm our view. It is therefore desirable to develop a different theoretical approach more appropriate to the analysis of such pulse sequences. Such a theory should provide a convenient way of expressing the effects of the rf-irradiation fields on the spin system. It should make it also possible to design new and more efficient composite pulses exploiting modulation of its amplitudes.

In this paper, it will be shown how the Floquet formalism satisfies many of these requirements for the two-level system which we will represent as a spin-$\frac{1}{2}$ interacting with rf irradiation. Previously, Maricq has demonstrated[30] that the Floquet formalism provides an alternative method equivalent to average Hamiltonian theory for the calculation of effective Hamiltonians of pulse cycles. Our version of the Floquet treatment, which is based on Shirley's perturbative approach,[31] is fundamentally different in its expression, and it is far from clear that a similar proof of its equivalence to either Maricq's treatment or AHT exists.

While the Floquet theory, like linear-response theory, is predicated on an initial step which expresses $\mathcal{H}(t)$, the time-dependent Hamiltonian, as a Fourier expansion, it makes no call to linear response and is more generally correct. We have previously demonstrated the use of Floquet theory in the prediction and explanation of a variety of nonlinear effects in NMR spectroscopy, including $N$-photon pulses.[32] Because the Floquet theory is designed explicitly for the analysis of periodic Hamiltonians, it is also ideally suited for the description of various magic-angle sample spinning (MASS) experiments.[33] In this paper we extend the application of the Floquet approach in order to treat arbitrary (but finite in time) irradiation sequences on two-level systems, and we apply that extension of the theory to the search for efficient broadband sequences where compensation for resonance offset

is accomplished by amplitude modulation of the irradiation. The same basic theory can also be applied to the problem of narrow-band excitation, and to broadband decoupling.

Much of this work has been influenced by an important recent paper of Shaka and Pines,[11] where they demonstrated a general approach to the design of broadband-excitation pulses using the machinery of average Hamiltonian theory. Their composite pulses are restricted to single-phase irradiation of constant strength (while alternating in amplitude between plus and minus). One question which one might ask is whether the restriction that the strength of the irradiation field is fixed unnecessarily increases the required irradiation power. On the face of it, it seems reasonable to expect that allowing amplitude modulation should reduce the required power, and perhaps significantly (as we have previously demonstrated elsewhere).[14] The Floquet approach provides the tools to find these phase- and amplitude-modulated pulses, and to optimize the efficiency of such pulses.

### B. Background to the Floquet formalism

The equation of motion for the density matrix $\rho$ which describes a time-dependent Hamiltonian $\mathcal{H}$ is given formally by

$$\frac{d\rho(t)}{dt} = -i[\mathcal{H}(t),\rho(t)] \ . \tag{1.1}$$

This equation has the formal solution

$$\rho(t) = U(0,t)\rho(0)U^{-1}(0,t) \ , \tag{1.2}$$

where $U(0,t)$, which is the propagator for $\rho$, satisfies the equation

$$\frac{d}{dt}U(0,t) = -i\mathcal{H}(t)U(0,t) \ , \tag{1.3}$$

with formal solution

$$U(0,t) = T\exp\left[-i\int_0^t \mathcal{H}(t')dt'\right] \ . \tag{1.4}$$

$T$ represents the Dyson time-ordering operator. Translating the rather simple formal solution represented by Eq. (1.4) into a useful solution is, however, a fairly difficult problem which has been extensively treated elsewhere in a variety of contexts. In NMR the treatment which is best known is average Hamiltonian theory.[27] The Floquet formalism provides an alternative approach to providing a useful solution. The heart of the formalism is a transformation which takes the time-dependent Hamiltonian $\mathcal{H}(t)$ into the time-independent Floquet Hamiltonian $H_F$. The operator $H_F$ has as its basis set all direct products of spin-state operators and Fourier-mode numbers. Because the Fourier-mode numbers can take on all possible values $-\infty \le n \le \infty$, $H_F$ is of infinite dimensionality. The evolution operator $U(0,t)$ is then given by

$$U_{pq}(0,t) = \sum_n \langle pn|e^{-iH_F t}|q0\rangle e^{in\omega t} \ . \tag{1.5}$$

Evaluation of Eq. (1.5) requires that $H_F$ be diagonalized. This is in itself a formidable task with no general solution. A computational approach may always be adopted; however, this severely restricts the opportunity to utilize theoretical insights. It is therefore of great importance to be able to perform at least part of the diagonalization procedure analytically.

In this paper we demonstrate how far in the analysis of amplitude-modulated irradiation sequences it appears possible to perform such a diagonalization. To do so, we introduce a set of infinite-matrix operators which simplify some subsequent mathematical manipulations. Using these operators we demonstrate the complete diagonalization of the Floquet Hamiltonian for linearly polarized irradiation sequences on resonance. In the more interesting case of off-resonance irradiation, preapplication of this diagonalizing transformation creates a new infinite matrix which is more readily suited to a treatment based on perturbation theory.

### C. Outline

The rest of this paper is organized as follows. In Sec. II we derive the Floquet approach to the description of two-level system evolution under time-dependent irradiation fields. Here we specialize to linearly polarized irradiation, although the more general case of arbitrary irradiation might also be treated (at the expense of considerable complication of some of the transformation expressions). In Sec. III the theory is applied to the problem of broadband excitation, and we derive a number of highly efficient sequences. A combination of the Floquet theory and perturbation theory is used to guide the numerical search which ultimately optimizes the detailed performance of the sequence. Methods of calculation of broadband pulse sequences are demonstrated, and evolution pathways during the irradiation sequence are shown. We comment on constraints on the design of low-power composite pulses using the Floquet formalism. Finally, some extensions of the theoretical approach are discussed. Experimental examples which verify the theoretical predictions as to efficiency and degree of compensation have already appeared elsewhere,[14] and although additional measurements where these results are exploited are in progress they will not be presented here.

## II. THE FLOQUET FORMALISM

In this section we describe the application of the Floquet formalism to the evaluation of the response of a spin system with spin $I=\frac{1}{2}$ to an arbitrarily shaped rf-irradiation sequence. To describe our theoretical approach, we first reintroduce the Floquet theory in a form convenient for the description of the spin $I=\frac{1}{2}$ system.[31,34] Then the elements of the evolution operator during rf irradiation can be reexpressed in terms of the Fourier components of the irradiation field and its off-resonance value. Finally, in Sec. III simple shapes will be deduced for pulses with broadband-excitation character. While the initial Fourier analysis of the pulse might suggest that the theory is a variation on the linear-response

approach, our treatment preserves the coherent nature of the problem and treats the interaction of the spin systems with all applied rf fields simultaneously and completely.

### A. The Floquet Hamiltonian

A spin system with an arbitrarily applied irradiation field can be represented by its spin Hamiltonian in the rotating frame (in frequency units) as

$$\mathcal{H}(t)=-\Delta\omega I_z+\omega^x(t)I_x+\omega^y(t)I_y\ , \tag{2.1}$$

where $\omega^x(t)$ and $\omega^y(t)$ are the time-dependent $x$ and $y$ components, respectively, of the irradiation sequence, and $\Delta\omega$ is the resonance offset of the irradiation. Where the sequence lasts a time $\tau$, a frequency parameter $\omega=2\pi/\tau$ can be defined. Expanding $\omega^x(t)$ and $\omega^y(t)$ in a Fourier series,

$$\omega^{x,y}(t)=\sum_{n=-\infty}^{\infty}\Omega_n^{x,y}\cos(n\omega t+\psi_n^{x,y})=\sum_{n=-\infty}^{\infty}\omega_n^{x,y}e^{in\omega t}\ , \tag{2.2}$$

where

$$\omega_n=\tfrac{1}{2}\Omega_n e^{i\psi_n}\ . \tag{2.3}$$

(While a number of rotating frames and thus resonance offsets may be defined, in this paper there will always be a "natural" rotating-frame representation where $\omega_n=\omega^*_{-n}$, and thus there will be no ambiguity.) The set of Fourier coefficients $\{\omega_n^x\}$ and $\{\omega_n^y\}$ contains all available information about the time-dependence of the irradiation sequence, and determines the elements of matrix representation of the Floquet Hamiltonian $H_F$. Its nonvanishing matrix elements are

$$\begin{aligned}
&\langle\alpha n|H_F|\alpha n\rangle=-\tfrac{1}{2}\Delta\omega+n\omega\ ,\\
&\langle\alpha n|H_F|\beta m\rangle=+\tfrac{1}{2}(\omega^x_{m-n}-i\omega^y_{m-n})\ ,\\
&\langle\beta_n|H_F|\beta n\rangle=+\tfrac{1}{2}\Delta\omega+n\omega\ ,\\
&\langle\beta n|H_F|\alpha m\rangle=\langle\alpha m|H_F|\beta n\rangle^*\ .
\end{aligned} \tag{2.4}$$

To simplify some important mathematical manipulations of this matrix which will allow us to evaluate the expression given in Eq. (1.5) for the evolution-operator matrix $U(0,\tau)$, we introduce here a set of new infinite matrix operators. Examples of these non-Hermitian operators are illustrated in Fig. 1, and have nonvanishing elements

$$\begin{aligned}
&\langle\alpha k|N|\alpha k\rangle=k,\quad \langle\beta k|N|\beta k\rangle=k\ ,\\
&\langle\alpha k|Z_m|\alpha k+m\rangle=\tfrac{1}{2},\quad \langle\beta k|Z_m|\beta k+m\rangle=-\tfrac{1}{2}\ ,\\
&\langle\alpha k|X_m|\beta k+m\rangle=\tfrac{1}{2},\quad \langle\beta k|X_m|\alpha k+m\rangle=\tfrac{1}{2}\ ,\\
&\langle\alpha k|Y_m|\beta k+m\rangle=-\frac{i}{2},\quad \langle\beta k|Y_m|\alpha k+m\rangle=\frac{i}{2}
\end{aligned} \tag{2.5}$$

for integer values of $k$. Reexpressing the Floquet Hamiltonian in terms of these parameters, $H_F$ takes on the simple form

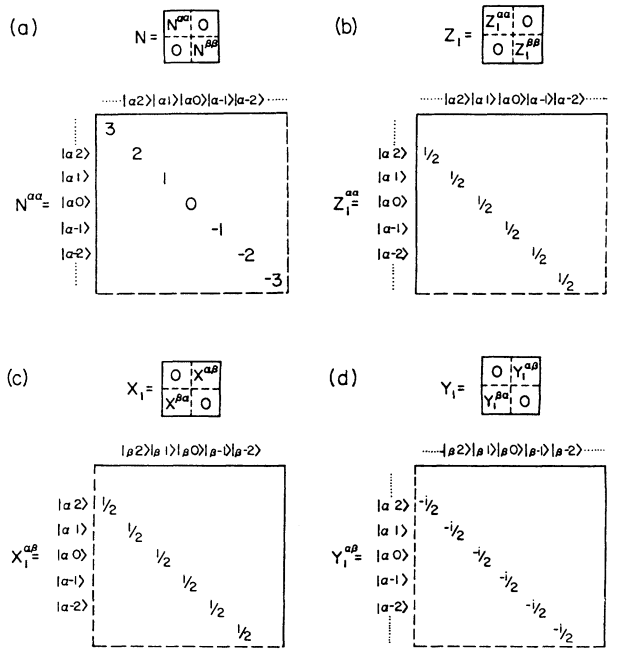


FIG. 1. Matrix representations of some of the infinite matrix operators $N$, $Z_i$, $X_i$, and $Y_i$ defined in Eq. (2.5). (a) The diagonal matrix $N$, where $\langle\alpha n|N^{\alpha\alpha}|\alpha n\rangle=\langle\beta n|N^{\beta\beta}|\beta n\rangle=n$. (b) The block-diagonal matrix $Z_1$, with $\langle\alpha n-1|Z_1^{\alpha\alpha}|\alpha n\rangle=-\langle\beta n-1|Z_1^{\beta\beta}|\beta n\rangle=\frac{1}{2}$. (c) The block off-diagonal matrix $X_1$, with $\langle\alpha n-1|X_1^{\alpha\beta}|\beta n\rangle=\langle\beta n-1|X_1^{\beta\alpha}|\alpha n\rangle=\frac{1}{2}$. (d) The block off-diagonal matrix $Y_1$, with $\langle\alpha n-1|Y_1^{\alpha\beta}|\beta n\rangle=-\langle\beta n-1|Y_1^{\beta\alpha}|\alpha n\rangle=-i/2$.

$$H_F=\omega N-\Delta\omega Z_0+\sum_n\omega_n^xX_n+\sum_n\omega_n^yY_n\ , \tag{2.6}$$

where the sums run over all values of $n$.

### B. The infinite operators

Simple commutation laws exist for these operators. They will prove of great assistance subsequently in the derivation of the expressions for $U(0,\tau)$, and therefore are provided here:

$$\begin{aligned}
&[X_n,X_m]=0,\quad [X_n,Y_m]=iZ_{n+m},\quad [X_n,N]=nX_n\ ,\\
&[Y_n,Y_m]=0,\quad [Y_n,Z_m]=iX_{n+m},\quad [Y_n,N]=nY_n\ ,\\
&[Z_n,Z_m]=0,\quad [Z_n,X_m]=iY_{n+m},\quad [Z_n,N]=nZ_n\ .
\end{aligned} \tag{2.7}$$

These operators are not Hermitian; to write $H_F$ as a sum of Hermitian operators we use the facts that $\omega^x_{-n}=(\omega_n^x)^*$ and $\omega^y_{-n}=(\omega_n^y)^*$. Then an equivalent form for $H_F$ would be

$$\begin{aligned}
H_F=\omega N-\Delta\omega Z_0&+\sum_n\mathrm{Re}(\omega_n^x-i\omega_n^y)P_n\\
&-\sum_n\mathrm{Im}(\omega_n^x-i\omega_n^y)Q_n\ ,
\end{aligned} \tag{2.8}$$

where the Hermitian operators $P_n$ and $Q_n$ have matrix elements

$$\langle \alpha k|P_m|\beta k+m\rangle=\langle \beta k+m|P_m|\alpha k\rangle=\tfrac{1}{2}\ ,$$
$$\langle \alpha k|Q_m|\beta k+m\rangle=\langle \beta k+m|Q_m|\alpha k\rangle^*=-\frac{i}{2}\ . \tag{2.9}$$

In most of our applications, it seems preferable to work instead with the non-Hermitian operators $X_n$, $Y_n$, and $Z_n$ described above.

The commutation relations provided above enable us to evaluate some useful transformations. Given the cyclic commutation relations $[X_0,Y_n]=iZ_n$ and $[X_0,Z_n]=-iY_n$, it is relatively simple to derive the transformation of $Y_n$ by $\exp(i\alpha X_0)$. Using the Taylor-series expansion for exponential operators, and for arbitrary operators $A$ and $B$, we have

$$e^{iA}Be^{-iA}=B+i[A,B]-\tfrac{1}{2}[A,[A,B]]-\frac{i}{3}[A,[A,[A,B]]]+\cdots\ . \tag{2.10}$$

For $A=\alpha X_0$ and $B=Y_n$, Eq. (2.10) simplifies to

$$e^{i\alpha X_0}Y_ne^{-i\alpha X_0}=\cos\alpha Y_n+\sin\alpha Z_n\ . \tag{2.11a}$$

Similarly,

$$e^{i\alpha Y_0}X_ne^{-i\alpha Y_0}=\cos\alpha X_n-\sin\alpha Z_n\ . \tag{2.11b}$$

Other useful transformations that follow from Eq. (2.10) include

$$e^{i\alpha X_n}Ne^{-i\alpha X_n}=N+i\alpha nX_n \tag{2.12a}$$

and

$$e^{i\alpha Z_n}Ne^{-i\alpha Z_n}=N+i\alpha nZ_n\ . \tag{2.12b}$$

We shall see how combinations of these transformations [Eqs. (2.11) and (2.12)] allow us to diagonalize $H_F$ in some simple cases.

### C. Diagonalization of $H_F$

In this section we specialize to $H_F$ where $\Delta\omega=0$ and the irradiation is linearly polarized. $H_F$ is then diagonalized by pretransforming, using Eqs. (2.11) and (2.12), via

$$e^{-i\pi Y_0/2}\left[\omega N+\sum_n\omega_n^xX_n\right]e^{i\pi Y_0/2}=\omega N+\sum_n\omega_n^xZ_n \tag{2.13a}$$

or

$$e^{-i\pi X_0/2}\left[\omega N+\sum_n\omega_n^yY_n\right]e^{i\pi X_0/2}=\omega N+\sum_n\omega_n^yZ_n\ . \tag{2.13b}$$

As a result of this transformation $H_F$ is block diagonal. (When neither $\{\omega_n^y=0\}$ nor $\{\omega_n^x=0\}$, a similar result might be achieved, but in this more general case the description of the transformation operator is significantly more complicated. We leave this possibility for later discussion elsewhere.) For concreteness we choose $\{\omega_n^y=0\}$. Since all $Z_n$ operators commute, we have further that

$$e^{i\alpha Z_n}Z_me^{-i\alpha Z_n}=Z_m\ . \tag{2.14}$$

This transformation enables us to diagonalize the block-diagram matrices generated by the transformations described in Eq. (2.13). The simple commutation relations between the $N$ and $Z_n$ operators, and Eq. (2.12b) allow us to write

$$\begin{aligned}H_d&=\exp\left[i\sum_m\alpha_mZ_m\right]\left[\omega N+\sum_n\omega_nZ_n\right]\times\exp\left[-i\sum_m\alpha_mZ_m\right]\\&=\omega N+\sum_n(i\alpha_n n\omega+\omega_n)Z_n\ ,\end{aligned} \tag{2.15}$$

where $H_d$ is the matrix resulting from this second transformation. The $\alpha_n$ coefficients are free parameters. Where $\Delta\omega=0$, we can choose the $\alpha_n$ coefficients such that

$$\alpha_n=-i\frac{\omega_n}{n\omega},\quad n\neq0 \tag{2.16}$$

and $H_d$ is diagonal. It takes on the particularly simple form

$$H_d=\omega N+\omega_0Z_0\ . \tag{2.17}$$

This further proves the important result that the infinite diagonal matrix derived from a block-diagonal matrix whose diagonal elements are given by $\omega N$ has elements equal to the diagonal elements of the original matrix. The eigenvalues of a block-diagonal matrix of the form $\omega N+\sum_n\omega_nZ_n$ are therefore $n\omega\pm\frac{1}{2}\omega_0$.

Summarizing these results, for $\Delta\omega=0$ the Floquet matrix for an arbitrary linearly polarized irradiation sequence can be diagonalized by applying the transformations of Eqs. (2.13)–(2.15), with values for $\alpha$ as given from Eq. (2.16) and

$$\exp\left[i\sum_m\alpha_mZ_m\right]\exp\left[-i\frac{\pi}{2}Y_0\right]\left[\omega N+\sum_n\omega_n^xX_n\right]\exp\left[i\frac{\pi}{2}Y_0\right]\exp\left[\sum_m\alpha_mZ_m\right]=\omega N+\omega_0Z_0\ . \tag{2.18}$$

The matrix which diagonalizes $H_F$ at the resonance condition $\Delta\omega=0$ can therefore be determined by substituting the values $-i(\omega_n/n\omega)$ for $\alpha_n$ in the exponential operators of Eq. (2.20). The elements of this matrix can be expressed compactly in terms of the Bessel functions. (We defer the derivation of this fact to Appendix A.) At this

point we continue our discussion with a derivation of the matrix elements of the propagator matrix, $U(0,\tau)$, in terms of the elements of the Floquet matrix.

### D. The evolution operator

For convenience we rewrite Eq. (1.5) which expresses the matrix elements of the $2\times2$ evolution matrix $U(0,\tau)$, and

$$U_{pq}(0,\tau)=\sum_n \langle pn|e^{-iH_F\tau}|q0\rangle e^{in\omega\tau}\ , \tag{2.19}$$

where $p,q=\alpha,\beta$ are the states of the two-level system, and $n$ is the Fourier mode index. The calculation of these matrix elements requires that $H_F$ be diagonalized.

We define a diagonalization matrix $T$. For $\Delta\omega=0$ we know that the eigenvalues of $H_F$ are $\lambda_n=n\omega\pm\lambda/2$. Thus the elements of the evolution operator are

$$U_{pq}(0,\tau)=\sum_{n,m}\langle pn|T^{-1}|\alpha m\rangle\langle\alpha m|T|q0\rangle e^{-i\lambda\tau/2}e^{-i(m-n)\omega\tau}+\sum_{n,m}\langle pn|T^{-1}|\beta m\rangle\langle\beta m|T|q0\rangle e^{i\lambda\tau/2}e^{-i(m-n)\omega\tau}\ , \tag{2.20}$$

with $TH_FT^{-1}=\Lambda$. The matrix $\Lambda$ is diagonal with elements

$$\begin{aligned}\langle\alpha n|\Lambda|\alpha n\rangle&=n\omega+\frac{\lambda}{2}\ ,\\ \langle\beta n|\Lambda|\beta n\rangle&=n\omega-\frac{\lambda}{2}\ .\end{aligned} \tag{2.21}$$

For times $n\omega\tau=2m\pi$ this expression can be simplified, and

$$U(0,\tau)=\begin{bmatrix}T^{\beta}_{\alpha\alpha} & T^{\beta}_{\alpha\beta}\\ T^{\beta}_{\beta\alpha} & T^{\beta}_{\beta\beta}\end{bmatrix}e^{i\lambda\tau/2}+\begin{bmatrix}T^{\alpha}_{\alpha\alpha} & T^{\alpha}_{\alpha\beta}\\ T^{\alpha}_{\beta\alpha} & T^{\alpha}_{\beta\beta}\end{bmatrix}e^{-i\lambda\tau/2}\ , \tag{2.22}$$

where

$$\begin{aligned}T^{r}_{pq}&=\sum_n\langle pn|T^{-1}|r0\rangle\sum_m\langle rm|T|q0\rangle\\ &=\sum_n\langle rn|T|p0\rangle^*\sum_m\langle rm|T|q0\rangle\ .\end{aligned} \tag{2.23}$$

Equation (2.23) holds because the elements of the $T$ matrix are correlated, and

$$\langle pn|T|qm\rangle=\langle pn+k|T|qm+k\rangle \tag{2.24}$$

for all $k$. Furthermore, $T$ is unitary and therefore

$$\sum_n\langle pn|T|qm\rangle^*\langle pn|T|qm+k\rangle=\delta_{k0}\ . \tag{2.25}$$

We define pulse parameters $t_1$ and $t_2$ such that

$$t_1=T^{\beta}_{\alpha\alpha}=\sum_n\langle\beta n|T|\alpha0\rangle\sum_m\langle\beta m|T|\alpha0\rangle^* \tag{2.26}$$

and

$$t_2=T^{\beta}_{\alpha\beta}=\sum_n\langle\beta n|T|\beta0\rangle\sum_m\langle\beta m|T|\alpha0\rangle^*\ . \tag{2.27}$$

For our two-level system $U(0,\tau)$ corresponds to a rotation of a magnetization vector. Evolution during a pulse of duration $\tau$ can always be expressed as an overall rotation through an angle $\gamma$ proportional to an effective field $H_{\rm eff}$ and the time $\tau$ about an axis of rotation defined by two polar angles $\bar\theta$ and $\bar\phi$. As $\bar\theta$ is conventionally defined as the rotation away from the $z$ axis, while most of our work is more naturally defined with respect to rotations away from the $x$-$y$ plane, we will use instead the angles $\theta=\pi/2-\bar\theta$ and $\phi=\bar\phi$. Figure 2 represents this rotation schematically. The evolution operator can then be expressed in terms of these rotation parameters and takes on the form

$$\begin{aligned}U(0,\tau)&=\begin{bmatrix}\cos^2(\bar\theta/2) & \frac{1}{2}(\sin\bar\theta)e^{i\bar\phi}\\ -\frac{1}{2}\sin\bar\theta e^{-i\bar\phi} & \sin^2(\bar\theta/2)\end{bmatrix}e^{i(\gamma/2)}+\begin{bmatrix}\sin^2(\bar\theta/2) & -\frac{1}{2}(\sin\bar\theta)e^{i\bar\phi}\\ \frac{1}{2}\sin\bar\theta e^{-i\bar\phi} & \cos^2(\bar\theta/2)\end{bmatrix}e^{-i(\gamma/2)}\\ &=\frac{1}{2}\begin{bmatrix}1+\sin\theta & (\cos\theta)e^{i\phi}\\ -(\cos\theta)e^{-i\phi} & 1-\sin\theta\end{bmatrix}e^{i(\gamma/2)}+\frac{1}{2}\begin{bmatrix}1-\sin\theta & -(\cos\theta)e^{i\phi}\\ (\cos\theta)e^{-i\phi} & 1+\sin\theta\end{bmatrix}e^{-i(\gamma/2)}\ .\end{aligned} \tag{2.28}$$

Comparing this result with Eq. (2.22) it becomes possible to express the elements $t_1$ and $t_2$ of the matrix which diagonalizes $H_F$ in terms of the rotation parameters which characterize the pulse, and

$$\begin{aligned}\lambda&=\frac{\gamma}{\tau}\ ,\\ t_1&=\cos^2(\bar\theta/2)=\tfrac{1}{2}(1+\sin\theta)\ ,\\ t_2&=\tfrac{1}{2}(\sin\bar\theta)e^{i\bar\phi}=\tfrac{1}{2}(\cos\theta)e^{i\phi}\ .\end{aligned} \tag{2.29}$$

Our procedure, which can be expressed in a few formal steps, leads to a calculation of the effective rotation parameters (which is equivalent to calculating the effective Hamiltonian) for a two-level system during application of a time-dependent field. First, we calculate the Floquet Hamiltonian and diagonalize it. The eigenvalues of $H_F$ determine the rotation angle $\gamma$, while the eigenvectors determine the axis of rotation and thus the angles $\theta$ and $\phi$. The object of the rest of this paper is therefore to ex-

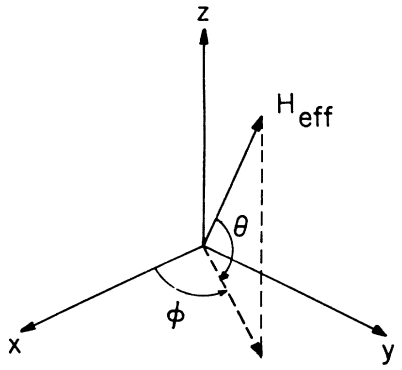


FIG. 2. Schematic representation of the effective field $H_{\text{eff}}$ in the rotating frame corresponding to a finite-irradiation field of effective flip angle $\gamma=|H_{\text{eff}}|\tau$. The direction of this field is defined by the polar angles $\bar{\theta}=\pi/2-\theta$ and $\bar{\phi}=\phi$.

plore strategies of achieving this diagonalization. As we are specifically interested in broadband-excitation pulses, we aim to generate sets of coefficients $\{\omega_n\}$ where the propagator $U(0,\tau)$ is independent of offset over a wide range of values $\Delta\omega$. Before continuing our derivation of the dependence of $U(0,\tau)$ on the coefficients $\{\omega_n\}$, we digress briefly and discuss some general features of rf pulses which will be important for our future discussion.

### E. rf pulses

The overall effect of any finite pulse can always be described via its propagator $U(0,\tau)$. For a two-level system it can also be visualized as the rotation of a vector on a globe about a second vector representing the effective field, as in Fig. 2. The interaction between the field and the system that this rotation represents is characterized both by parameters of the field, including the length, the intensity(ies) and the phase(s) of the components of the irradiation, and further by the offset from resonance $\Delta\omega$ characteristic of the system. A composite pulse with broadband-excitation character corresponds to a very special set $\{\omega_n\}$, such that the dependence of $\gamma$, $\theta$, and $\phi$ is largely independent of $\Delta\omega$. In contrast, in narrow-band pulses one attempts to ensure that the dependence of $U(0,\tau)$ on $\Delta\omega$ is so strong that the propagator differs from the unit matrix for only some small range of offset values (narrow-band excitation), or else so that it is the unit matrix for some fixed value of offset only (solvent suppression). For most composite pulse sequences, numerical methods ultimately must be exploited to optimize behavior for the desired dependences.[11,35,36]

In many practical cases the pulse intensities are kept constant while the desired improvement is obtained by increasing the total length of the pulse sequence, perhaps by repeating the same pulse sequence with the phases changed so that errors in the supercycle cancel rather than propagate. Very generally, as the pulse sequence increases in length the degree of compensation can be made higher and thus the results appear more satisfactory. Similarly, superficially superior results are trivially achieved by simply increasing the strength of a given irradiation field without similarly increasing the scale of offsets $\Delta\omega$. So as to place all pulse sequences on an equivalent quality scale, the results of compensated pulse sequences are generally described in terms of a dimensionless bandwidth unit $\Delta\omega_1/\omega_1$ (for compensation of rf inhomogeneity) or $\Delta\omega/\omega_1$ (for compensation of resonance offset). Where the field amplitude is not fixed in time, it is more correct to consider the parameter $\Delta\omega/\bar{\omega}$ where $\bar{\omega}$ corresponds to the root-mean-square field intensity. Where no amplitude modulation is allowed, $\bar{\omega}=\omega_1$. While from a theoretical perspective the power required to achieve a given bandwidth is irrelevant, it is nonetheless of considerable importance at a practical level to design pulses with broad bandwidths at low powers. Because the maximum field is limited in any laboratory situation, in any amplitude modulated pulse we will also take note of $\omega_{\max}$, the maximum rf field required in any pulse cycle. If we fix the pulse sequence length $\tau$, then $\omega_1$ is the only free parameter and $\bar{\omega}$ becomes a further measure of the relative qualities of broadband-pulse sequences with equivalent bandwidth. Long composite pulses composed of $n$ subcycles have values of $\bar{\omega}$ which are $n$ times as large as that of the subcycle itself. Our goal is to design sequences with small values of $\bar{\omega}$ which nonetheless are compensated to large values of $\Delta\omega/\bar{\omega}$. Where the maximum offset at which satisfactory compensation is achieved is $\Delta\omega_{\max}$, the bandwidth is given by $\overline{\Delta\omega_{\max}}=\Delta\omega_{\max}/\bar{\omega}$.

The restriction in this paper to linearly polarized fields is made so as to simplify the mathematical treatment. We have previously discussed $N$-photon pulses, which are one special case of pulses where irradiation is simultaneously applied along both $x$ and $y$ axes.[32] A more general treatment of such irradiation sequences will follow in a later publication.

### F. On-resonance irradiation

The response of a two-level system is to a linearly polarized irradiation field of time-dependent intensity $\omega_x(t)$. Where the resonance offset $\Delta\omega=0$, the Dyson time-ordering operator $T=1$. Then $U(0,\tau)$ can easily be evaluated by direct integration of Eq. (1.4) and

$$\begin{aligned}U(0,\tau)&=\exp\left[-i\int_0^{\tau}\mathcal{H}(t')dt'\right]\\&=\frac{1}{2}\begin{bmatrix}1&1\\-1&1\end{bmatrix}e^{i\omega_0\tau}+\frac{1}{2}\begin{bmatrix}1&-1\\1&1\end{bmatrix}e^{-i\omega_0\tau}\\&=e^{-i\gamma I_x}\,,\end{aligned}\tag{2.30}$$

where the pulse parameters are

$$\gamma=\int_0^{\tau}\omega(t)dt,\quad \theta=0^\circ,\quad \phi=0^\circ\,.\tag{2.31}$$

The root-mean-square power in the pulse is given by

$$\bar{\omega}=\left[\frac{1}{\tau}\int_0^{\tau}\omega^2(t)dt\right]^{1/2}\tag{2.32}$$

and its maximum intensity by

$$\omega_{\max}=\max\{\omega(t)\}_0^{\tau}\,.\tag{2.33}$$

This simple solution for $U(0,\tau)$ for a linearly polarized irradiation sequence should, of course, also be obtained from the Floquet formalism we have presented above. For this simple case it may appear that the derivation of the elements of $U(0,\tau)$ using the Floquet formalism is, in fact, unnecessary. Nonetheless, we present this derivation in order to establish the theoretical framework for the treatment of the more interesting case of off-resonance irradiation.

The Floquet Hamiltonian $H_F$ is

$$H_F=\omega N+\sum_n \omega_n X_n \ , \tag{2.34}$$

where, as previously, we have reexpressed

$$\omega(t)=\sum_n \omega_n e^{in\omega t} \ . \tag{2.35}$$

An alternative expression for Eq. (2.32) is

$$\bar{\omega}=\left[\frac{1}{\tau}\left[\omega_0^2+\tfrac{1}{2}\sum_{n\neq 0}\omega_n^2\right]\right]^{1/2} \ . \tag{2.36}$$

Using the results of Sec. II D, $H_F$ can be immediately diagonalized and

$$DH_FD^{-1}=\omega N+\omega_0 Z_0 \ , \tag{2.37}$$

where

$$D=\exp\left[\sum_{n\neq 0}\frac{\omega_n}{n\omega}Z_n\right]\exp\left[-i\frac{\pi}{2}Y_0\right] \ . \tag{2.38}$$

The elements of the unitary matrix $D$ depend on one another, and

$$\begin{aligned}&\langle \alpha n|D|\alpha m\rangle=\langle \alpha n|D|\beta m\rangle \ ,\\ &-\langle \beta n|D|\alpha m\rangle=\langle \beta n|D|\beta m\rangle \ ,\end{aligned} \tag{2.39}$$

which we derive from the fact that $\exp[\sum_n(\omega_n/n\omega)Z_n]$ is block diagonal, and $\exp(-i\pi Y_0/2)$ is a simple infinite matrix with values $1/\sqrt{2}$ at the diagonal elements of three of its four subblock matrices, and $-\frac{1}{52}$ at the diagonal of the fourth. Furthermore, it is shown in Appendix B that

$$\sum_n\langle \alpha n|D|\alpha 0\rangle=\sum_n\langle \alpha n|D|\beta 0\rangle=\frac{1}{\sqrt{2}} \ . \tag{2.40}$$

Combining these results with the results of Eq. (2.29), and where $D=T$, the evolution matrix $U(0,\tau)$ for $\Delta\omega=0$ is identical to that of Eq. (2.31). The diagonalization matrix of Eq. (2.38) will prove of much importance in our subsequent discussion of the case of off-resonance irradiation. Where the elements of $D$ are needed they can be calculated using the definitions of the $Z_n$ operators and the Taylor-series expansion for the exponentials of operators. Somewhat later in our discussion, an example of a calculation of these elements will be performed. Instead, here we continue our discussion of how one extends the Floquet formalism so as to obtain the pulse parameters $\gamma$, $\theta$, and $\phi$ in the more general case of off-resonance irradiation. Here we restrict ourselves to broadband-excitation pulses only; in subsequent publications we will treat the possibility of other types of excitation. Again, our goal is to diagonalize the Floquet matrix and then use the expression Eqs. (2.29) and (2.31) so as to solve for the pulse parameters which provide us with the effective Hamiltonian. In the absence of a general analytic diagonalization procedure, the application of perturbation theory will be explored.

### G. Off-resonance irradiation

Irradiation pulses of finite length $\tau$ and intensity on resonance of $\omega_0$ can be modified so as to become broadband-excitation pulses by changing the shape of the pulse or by applying phase shifts to the pulse. We focus on the former possibility, and aim to choose amplitudes $\omega_n$ such that $\gamma\approx\omega_0\tau$, $\theta\approx 0°$, and $\phi\approx 0°$ for $\Delta\omega\neq 0$. In language more adapted to the Floquet formalism, a broadband-irradiation sequence is found when the eigenvalues of the $H_F$ matrix $\lambda_n=n\omega\pm\frac{1}{2}\lambda$ are approximately constant independent of $\Delta\omega$, and therefore neither the $t_1$ nor $t_2$ parameters depend strongly on offset. Such pulses are broadband in the sense that $U(0,\tau)$ is independent of $\Delta\omega$ over some range of offsets. [Special broadband pulses also exist which, despite the fact that the propagator may depend on offset, transform particular initial states of the density operator $\rho(0)$ into particular final states $\rho(t)$ independent of $\Delta\omega$. While certain of these pulses have been derived from our efforts,[14(a),14(b)] the Floquet formalism, which operates on the propagator without reference to the initial and/or final states, provides little guidance in discovering such sequences. We therefore confine our discussion here to such sequences where the propagator itself is broadband.]

Where irradiation is applied only along the $x$ axis in the rotating frame, the Floquet Hamiltonian can be written

$$H_F=-\Delta\omega Z_0+\omega N+\sum_n \omega_n X_n \ . \tag{2.41}$$

We divide the diagonalization procedure which will lead to the eigenvalues and eigenvectors of $H_F$ into two distinct steps. First, we transform $H_F$ via the $D$ operator of Eq. (2.38). This results in

$$H_d=DH_FD^{-1}=\omega N+\omega_0 Z_0+\Delta\omega\Delta \ , \tag{2.42}$$

where $\Delta$ is a matrix given by

$$\Delta=DZ_0D^{-1} \ . \tag{2.43}$$

The $\Delta$ matrix has the same general form as all other Hermitian matrices in the Floquet manifold with nonzero elements

$$\langle \alpha 0|\Delta|\beta n\rangle=\langle \alpha k|\Delta|\beta n+k\rangle=\delta_n \ , \tag{2.44a}$$

$$\langle \beta 0|\Delta|\alpha n\rangle=\langle \beta k|\Delta|\alpha n+k\rangle=\delta^*_{-n} \ . \tag{2.44b}$$

The set of coefficients $\{\delta_n\}$ defines the matrix elements of the off-diagonal block $\Delta$. The expression for the transformed Hamiltonian $H_d$ is conveniently designed for the application of perturbation theory at small offsets, $\Delta\omega$. At small-enough offsets, Eq. (2.42) is nearly diagonal

with eigenvalues given by Eq. (2.21). Where a pulse is broadband the eigenvalues of $H_F$ vary little from these values, even where $\Delta\omega$ may be significantly different from zero. To accomplish this, perturbation theory suggests that it is necessary to find some combination of $\omega_n$, such that the elements of $\Delta$ are uniformly smaller than the differences between their corresponding diagonal values, $|\delta_n| \ll (n\omega - \omega_0)$. Satisfying this condition in a systematic way requires that we first derive the dependence of the values $\delta_n$ on $\omega_n$.

### H. The Δ matrix

As defined in Eq. (2.43) the $\Delta$ matrix is given by

$$\Delta = \exp\left[\sum_n \frac{\omega_n}{n\omega} Z_n\right] \exp\left[-i\frac{\pi}{2} Y_0\right] Z_0 \exp\left[i\frac{\pi}{2} Y_0\right] \times \exp\left[-\sum_n \frac{\omega_n}{n\omega} Z_n\right] . \tag{2.45}$$

Nonzero elements of $\Delta$ exist only between the $\alpha$ and $\beta$ manifolds of states.

A schematic representation of the matrix $\Delta$ is given in Fig. 3. The elements $\delta_n$ can be derived from the definitions of $X_n$, $Y_n$, and $Z_n$ operators given in Eq. (2.8). Using these definitions, and that the exponential coefficients $[(\omega_n/n\omega)Z_n]$ commute with one another, the $\delta_n$ values may be obtained by a straightforward multiplication of the matrices corresponding to the individual exponents. A derivation for a general expression useful for calculating the $\delta_n$ is given in Appendix A.

Here we provide an explicit example for the case of irradition with one, two, and three modulation frequencies only, say, $\omega t$, $2\omega t$, and $3\omega t$. The full Hamiltonian $\mathcal{H}(t)$ is given by

$$\mathcal{H}(t) = -\Delta\omega I_z + H(t) , \tag{2.46a}$$

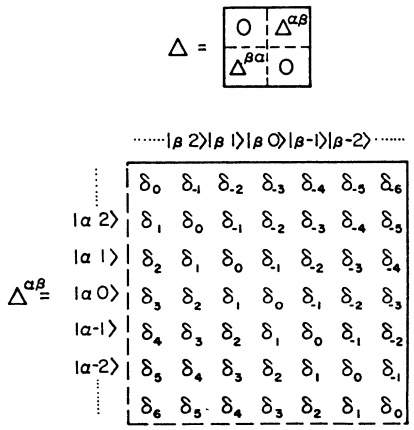


FIG. 3. Matrix representation of the Hermitian operator $\Delta$ with elements $\delta_n$ as defined in Eq. (2.45). The elements of the two submatrices $\Delta^{\alpha\beta}$ and $\Delta^{\beta\alpha}$ are correlated such that $\langle \beta m - n|\Delta^{\beta\alpha}|\alpha m\rangle = \langle \alpha m|\Delta^{\alpha\beta}|\beta m - n\rangle^* = \delta^*_n$.

where $H(t)$, the time-dependent portion of $\mathcal{H}$, is

$$H(t) = [\omega_0 + \Omega_1\cos(\omega t + \psi_1) + \Omega_2\cos(2\omega t + \psi_2) + \Omega_3\cos(3\omega t + \psi_3)]I_x , \tag{2.46b}$$

and $\omega_0\tau$ is the flip angle on resonance. The $\Delta$ matrix depends explicitly on only $H(t)$. For $\Omega_2 = \Omega_3 = 0$,

$$\delta_n = -\tfrac{1}{2} J_n\left(\frac{\Omega_1}{\omega}\right) e^{in\psi_1} . \tag{2.47}$$

The expressions for two and/or three modulation fields are somewhat more complicated, and for two fields

$$\delta_n = -\tfrac{1}{2}\sum_k J_{n-2k}\left(\frac{\Omega_1}{\omega}\right) J_k\left(\frac{\Omega_2}{2\omega}\right) e^{i[(n-2k)\psi_1 + k\psi_2]} , \tag{2.48a}$$

while adding a third field at frequency $3\omega t$,

$$\delta_n = -\tfrac{1}{2}\sum_{k,l} J_{n-2k-3l}\left(\frac{\Omega_1}{\omega}\right) J_k\left(\frac{\Omega_2}{2\omega}\right) J_l\left(\frac{\Omega_3}{3\omega}\right) \times e^{i[(n-2k-3l)\psi_1 + k\psi_2 + l\psi_3]} . \tag{2.48b}$$

The $\delta_n$ elements are relatively simple functions of the Fourier components of the irradiation. Products of the Bessel functions are easily calculated, and the values of $\delta_n$ provide a complete and exact representation of the time dependence of the irradiation in the Floquet formalism. Several interesting aspects of Eqs. (2.47) and (2.48) (and the more general equations of Appendix A) should be pointed out. The sensitivity of $\delta_n$ to $\Omega_k$ decreases for increasing $k$ because the argument of the Bessel function is $(\Omega_k/k\omega)$. This suggests that while each of the nonzero $\Omega_k$ coefficients contributes to every one of the $\delta_n$ matrix elements, the values of the $\delta_n$ depend most critically on the lowest-order coefficients, say, $\Omega_1$ and $\Omega_2$. The $\delta_n$ are less sensitive to the precise value of higher-order coefficients. Furthermore, the $\Delta$ matrix is independent of $\omega_0$, and thus characteristic exclusively of the details of the modulation scheme; $\omega_0$ appears only in the diagonal blocks of $H_F$.

Before leaving our description of $H_F$, we mention some further properties of the $\Delta$ matrix which severely constrain the allowed values of the $\delta_n$. These properties are derived in Appendix B, and because they have important consequences for the derivation of specialized irradiation schemes, they are presented here. Constraints on the $\delta_n$ include

$$\sum_n |\delta_n|^2 = \tfrac{1}{4} , \tag{2.49a}$$

$$\sum_k \delta_n \delta^*_{n+k} = 0, \quad k \neq 0 \tag{2.49b}$$

and, using the arguments of Appendix B,

$$\left|\sum_n \delta_n\right| = \tfrac{1}{2} . \tag{2.49c}$$

These three conditions greatly restrict the possible values of the $\delta_n$. While it might appear logical to design pulse

sequences by building up a matrix $\Delta$ with appropriate properties, the constraints represented by Eq. (2.49) and the practical difficulty involved in inverting Eqs. (2.47) or (2.48) make this method less attractive. We instead emphasize the role of the $\omega_n$ or the $\Omega_n$, which are unconstrained.

In this section we have demonstrated the procedure by which the matrix elements of the Floquet Hamiltonian are derived. Given a set of Fourier coefficients $\omega_n$ describing the time dependence of a linearly polarized irradiation sequence, we can calculate the $\delta_n$ values which characterize the $\Delta$ submatrix. These values can then be used with Eq. (2.39) to form the transformed Hamiltonian $H_d$. Diagonalization of this Hamiltonian will provide the eigenvalues $\lambda_m$, and from the elements of the diagonalization matrix we can evaluate $t_1$ and $t_2$ and thus derive the angular factors $\theta$ and $\phi$ which complete the description of $U(0,\tau)$.

Having completed our description of the Floquet Hamiltonian and demonstrated the calculation of its matrix elements, in Sec. III we address the central question of diagonalizing $H_F$ and designing irradiation sequences that satisfy particular properties. Where an analytic diagonalization is not possible, approximate methods must be developed. For broadband excitation, the off-diagonal elements $\Delta\omega\delta_n$ can always be made small enough so that the diagonalization of $H_F$ can be addressed by a perturbation treatment. This is particularly so because in the case of broadband-excitation pulses the eigenvalues of the transformed matrix $DH_FD^{-1}$ are independent of $\Delta\omega$ and approximately equal to the original values $n\omega\pm\frac{1}{2}\omega_0$ over a wide range of offsets. This suggests that the matrix which diagonalizes $H_d=DH_FD^{-1}$ for a broadband-pulse sequence should differ only slightly from the unity matrix, and therefore justifies the use of perturbation theory. For other classes of pulses (e.g., narrow-band or selective irradiation) other approaches will certainly be required.

## III. BROADBAND EXCITATION

### A. Design considerations

We henceforth model our two-level system as a magnetization vector precessing about a near-resonant rf field. A broadband-excitation pulse is defined by the property that at the end of the broadband pulse and for some range of offsets $\Delta\omega<\Delta\omega_{\max}$ such a magnetization vector is rotated a fixed angle $\gamma$ about a constant rotation axis given by $\theta$ and $\phi$. Note that the broadband character is defined without reference to the details of the pathway traversed during the pulse. For a finite pulse with on-resonance rotation angle $\gamma_0$ and where the direction angles $\theta_0=\phi_0=0$ describe $H_{\text{eff}}$ for $\Delta\omega=0$, our goal is to find Fourier coefficients $\{\omega_n\}$ such that the values of $\gamma$, $\theta$, and $\phi$ are independent of $\Delta\omega$. In the language of the Floquet theory, the eigenvalues of the Floquet Hamiltonian should be given by $\lambda=\omega_0/2$, while $t_1=t_2=\frac{1}{2}$ for $\Delta\omega\neq 0$. We seek some set of values $\delta_n$ in the transformed Hamiltonian $H_d$ of Eq. (2.39), which leave its diagonal part unchanged for $\Delta\omega\neq 0$; that is,

$$D_1H_dD_1^{-1}=D_1(\omega_0Z_0+\omega N+\Delta\omega\Delta)D_1^{-1}\approx\omega_0Z_0+\omega N\ , \tag{3.1}$$

where $D_1$ represents the transformation matrix which diagonalizes $H_d$. This matrix is related to the $T$ and $D$ matrices of Eqs. (2.20) and (2.38), and

$$T=D_1D\ . \tag{3.2}$$

Perturbation theory should be applicable to the calculation of $D_1$ if we expect that the eigenvalues $\lambda_n$ of $D_1H_dD_1^{-1}$ are nearly constant over some large range of offsets $\Delta\omega$. First we derive an expression for the evolution frequencies $\lambda$. Subsequently, we consider the minimization of the deviations in the angles $\theta$ and $\phi$.

#### 1. *Approximate expressions for the evolution frequency*

As the elements of $\Delta$ are all off diagonal and, for $0<\omega_0<\omega$, i.e., for $0<\gamma<2\pi$, the diagonal elements of $H_d$ are nondegenerate, at small values of $\Delta\omega|\Delta|$ we can apply standard nondegenerate perturbation theory to the calculation of $\lambda_n$. Realizing that the elements $\delta_n$ of $\Delta$ couple diagonal elements whose differences are $n\omega+\omega_0$, we find

$$\lambda_n=n\omega\pm\frac{\lambda}{2}=n\omega\pm\tfrac{1}{2}[\omega_0+c_2(\Delta\omega)^2+c_4(\Delta\omega)^4+\cdots]\ , \tag{3.3a}$$

with

$$c_2=\sum_n\frac{\delta_n\delta_n^*}{n\omega+\omega_0} \tag{3.3b}$$

and[37]

$$c_4=\sum_{\substack{n,k,l\\k\neq l}}\frac{\delta_k\delta_l^*\delta_m\delta_{k-l+m}^*}{(k\omega+\omega_0)[(k-l)\omega][(k-l+m)\omega+\omega_0]}$$
$$-c_2\sum_n\frac{\delta_n\delta_n^*}{(n\omega+\omega_0)^2}\ . \tag{3.3c}$$

These are the standard expressions for the second- and fourth-order energy corrections from perturbation theory. We expect no odd-order corrections because where only linearly polarized irradiation is allowed, symmetry demands that $\lambda$ is independent of the sign of $\Delta\omega$. The expressions for $c_2$ and $c_4$ can be evaluated numerically starting from the $\omega_n$ or $\Omega_n$ values and Eq. (A9) of Appendix A, which allows us to calculate the $\delta_n$. As we do not know the precise values of $\delta_n$, it may be impossible to predict *a priori* the range of convergence over $\Delta\omega$ of any perturbation expansion. Nonetheless, it seems reasonable to assume that as long as $\lambda_n\approx n\omega\pm\omega_0/2$ and $D_1\approx 1$ this theory is valid. These are precisely the conditions which guarantee broadband excitation.

#### 2. *Approximate expression for the rotation axis*

The procedure described above, which guarantees that deviations from $\lambda_n$ are minimized for small offsets, is still

not a sufficient condition to guarantee that we have designed an acceptable broadband sequence. Minimization of $c_2$ and $c_4$ minimizes only the deviations in the eigenvalues, and thus $\gamma$, from the ideal values. In our broadband sequences we further require that the rotation direction varies only slowly with $\Delta\omega$, and thus that $D_1 \approx 1$. To satisfy this condition, we need also develop an approximate expression for $D_1$.

The diagonalization matrix $D_1$ represents the deviation of the matrix $T$ which diagonalizes $H_F$ from the transformation matrix $D$ which diagonalizes $H_F$ for $\Delta\omega=0$. For $D$ itself $t_1=t_2=\frac{1}{2}$, and therefore $\theta=0°$ and $\phi=0°$ [see Eqs. (2.27) and (2.28)]. Any deviation of $T$ from $D$, represented by the $D_1$ operator, modifies these values of $t_1$ and $t_2$, and therefore of $\theta$ and $\phi$. $D_1$ represents a tilt in the direction of the effective irradiation field out of the $x$-$y$ plane, and a rotation of the effective irradiation field away from the $x$ axis. This further constrains acceptable values of $\Omega_n$ and $\psi_n$ to those which satisfy $D_1 \approx 1$. We can guarantee that the polar angle $\phi$ is independent of $\Delta\omega$ is by choosing to work exclusively with pulses which are symmetric in time with respect to their centers, i.e., $\psi_n=0$ or $\pi$.[10,11,36] Then only the tilt angle $\theta$ is relevant. While the theory is independent of this simplification, we have usually chosen to explore only such pulses.

Generally, we can again use an approximate calculation to estimate the elements of $D_1$.[38] We define a Hermitian matrix $S$ such that

$$D_1 = e^{-iS} \approx 1 - iS \ . \tag{3.4}$$

We consider only the first-order term in the expansion of the exponent. The nonzero elements of $S$ are, to first order, proportional to the off-diagonal elements of $H_d$ in Eq. (3.1):

$$\langle \alpha k|S|\beta n+k\rangle = \frac{\langle \alpha k|\Delta|\beta n+k\rangle}{n\omega+\omega_0}\Delta\omega \tag{3.5}$$

and are therefore approximately proportional to both $\delta_n$ and $\Delta\omega$. Ideally, $S=0$. A relative measure of the magnitude of the $S$ matrix elements can be defined analogously to $t_1$ from Eq. (2.27) and we define $s_1$ such that

$$s_1 = \sum_n \langle \alpha n|S|\beta 0\rangle = \sum_n \frac{\delta_n}{n\omega+\omega_0} \ . \tag{3.6}$$

Minimization of $s_1$ minimizes the deviations in $\theta$ and $\phi$ from $\theta_0$ and $\phi_0$, to low order.

### B. Single-frequency modulation schemes

As an example of the application of Eqs. (3.3) to (3.6) we direct our attention to the problem of broadband pulses designed with only a single-modulation sideband (i.e., irradiation at a frequency $\pm m\omega$ with amplitude $\Omega_m$). First we demonstrate the application of the Floquet formalism to the problem of broadband 180° pulses in some detail. Then we will generalize to other flip angles before continuing in Sec. III C with a discussion of the generalization to multifrequency-irradiation schemes with superior properties, where the successful application

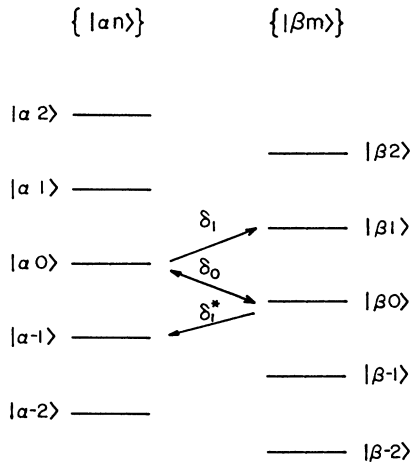


FIG. 4. Energy-level diagram representation of the transformed matrix $H_d=DH_FD^{-1}$. The diagonal matrix elements corresponding to the states $|\alpha n\rangle$ are separated from those of the states $|\beta n\rangle$ by $\omega_0=\omega/2$ for a pulse of length $\gamma_0=180°$. The off-diagonal elements $\delta_n$ of $H_d$ couple the states $|\alpha m\rangle$ with $|\beta m-n\rangle$. Diagonalization of $H_d$ results in a set of mixed states which are linear combinations of the $|\alpha n\rangle$ and $|\beta n\rangle$ states, with mixing coefficients dependent on the values of the $\delta_n$ coefficients. Broadband pulses are achieved when the mixing coefficients are all nearly 0 or 1 for large values of $\Delta\omega$.

of our theory requires extensive computer assistance.

For a broadband 180° pulse, the Hamiltonian is

$$\mathcal{H}(t)=[\omega_0+\Omega_m\cos(m\omega t+\psi_m)]I_x+\Delta\omega I_x \ , \tag{3.7}$$

where $\omega_0=\omega/2$. (Similarly, for a 90° pulse, $\omega_0=\omega/4$, and so on, for other flip angles.) The energy-level scheme which describes $H_F$ is shown in Fig. 4. The $\{|\alpha m\rangle\}$ manifold of states is shifted by $\omega/2$ in energy from the $\{|\beta m\rangle\}$ manifold. One solution for $\{\delta_n\}$ which sets $c_2=0$ is $|\delta_n|=|\delta_{-(1+n)}|$ for all $n$, because the denominators in Eq. (3.3b) are then successively equal and of opposite sign, while the numerators are equal, and therefore the sum of each pair of terms in the infinite series is zero.

Inspection of the expressions for $\delta_n$ of Appendix A shows that, for single-frequency irradiation at frequency $m\omega$, the only nonzero $\delta_n$ are for $n=pm$ for $p$ an integer. Furthermore, for single-frequency irradiation, $|\delta_n|=|\delta_{-n}|$ for all $n$. We can arrive at an approximate value of $\Omega_1$, such that $c_2=0$, by evaluating only the leading terms in the infinite series, i.e., those with the smallest denominators. This suggests an initial choice of $n=1$ in Eq. (3.7) and examining Eq. (3.3b) we choose as a initial approximation $|\delta_0|=|\delta_{-1}|$. Where $J_0(x)\approx J_1(x)$ for $x=\Omega_1/\omega$, we have an approximate single-frequency broadband $\pi$ pulse. There are an infinite number of solutions to this problem; the first two are $x\approx 1.43$ and $x\approx 4.68$. We expect solutions to $c_2=0$ to be found near these values of $x$. The lowest-amplitude solution is to be preferred, both because $\bar{\omega}$ is smaller and because the $\delta_n$ for $|n|>1$ are smaller for $x$ small. Thus we expect the convergence of the infinite series for $c_2$ to be more rapid. For $x<1.43$, $|\delta_0|>|\delta_1|$.

The leading terms for $c_4$ are similarly expressed. We consider only those terms in Eq. (3.3c) composed of products of $\delta_0$ and $\delta_{\pm 1}$. For the special case of single-frequency modulation, $\delta_0 = \delta_0^*$ and $\delta_{-1} = -\delta_1 \exp(-2i\psi_1)$, and we find

$$c_4 = -\tfrac{4}{3}\delta_0^2\delta_1\delta_1^* + \cdots . \tag{3.8}$$

The first term in our expression for $c_4$ is zero where $J_0(x)=0$ ($x \approx 2.4$) or $J_1(x)=0$ ($x=0$ or $x \approx 3.83$). As none of these conditions simultaneously satisfies $c_2 \approx 0$, broadband 180° pulses cannot be expected to be effective for large offsets with only single-frequency irradiation.

As a practical matter, higher-order corrections to the expansions for $c_2$ and $c_4$ change somewhat the precise numerical values cited above, although not the general conclusions. Numerical calculations show that the first zero in $c_2$ occurs at $x \approx 1.58$, and in $c_4$ at $x \approx 2.50$. Where minimization of the initial deviation in the overall rotation angle $\gamma$ from the ideal evolution frequency $\gamma_0$ is the sole criterion, $\Omega_1 \approx 1.58\omega$ provides the best composite 180° pulse. As predicted by Eq. (3.3), and illustrated in Fig. 5, the deviation in $\lambda$ is quartic in small offsets $\Delta\omega$ for this choice of $\Omega_1$. The effective bandwidth of such a pulse is, however, somewhat limited. Where the criterion is that the deviation $\Delta\gamma$ is small, broader bandwidths will be achieved for other values of $\Omega_1$. In particular, since $J_0$ and $J_1 > 0$, as long as $x < 1.58$, $c_2$ is positive while $c_4$ is negative. Therefore, for fields weaker than $x < 1.58$, there exists some offset $\Delta\omega \neq 0$ where $\Delta\gamma = 0$. A superior single-frequency 180° pulse is expected for $\Omega_1 < 1.58\omega$.

The procedure described above, which guarantees that deviations from $\gamma_0$ are minimized for small offsets, is, as discussed above, not sufficient to guarantee that we have designed an acceptable broadband sequence. We further require that the rotation direction vary only slowly with $\Delta\omega$, and thus that $D_1 \approx 1$. Therefore, we now turn our attention to our approximate expression for $D_1$, and therefore to the minimization of $s_1$.

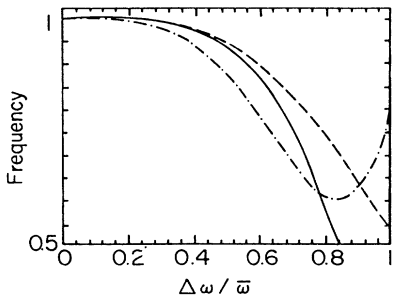


FIG. 5. Dependence of the normalized eigenvalue parameter $\lambda/\lambda_0$ as function of the resonance offset parameter $\Delta\omega/\bar{\omega}$ for single-frequency pulses of 90° and 180°. The single amplitudes $a_1$ were chosen to make $c_2=0$. The dashed line (— — —) corresponds to a 90° pulse with $a_0=\frac{1}{4}$ and $a_1=-1.57$; the dot-dashed line (—·—·—·) corresponds to a 180° pulse with $a_0=\frac{1}{2}$ and $a_1=-2.01$. The solid line (——) is the quartic function $\lambda/\lambda_0=[1-(\Delta\omega/\bar{\omega})^4]$. The initial decay for both of the pulses follows closely the model function, demonstrating their weak dependence on $\Delta\omega$ for small offsets.

Using approximate arguments such as those applied above, we initially consider only the largest terms in Eq. (3.6). This leads us to expect that the minimum value of $s_1$ will be found where $\delta_0 \approx \delta_{-1}$. Conveniently, this is a solution for $c_2=0$ as well. It additionally provides us with a constraint on the phase angle $\psi_1$. Using the general expressions for the $\delta_m$ from Appendix A, and the identity $J_{-n}(x)=(-1)^n J_n(x)$ we find that $\psi_1=\pi$ is the preferred choice. Including subsequent terms in the expansion, a more accurate calculation shows that the zeros of $s_1$ and $c_2$ are not identical. The minimum value in $s_1$ for single-frequency irradiation occurs at $x \approx 1.18$ and $\psi_1=\pi$.

As the minima $s_1$, $c_2$, and $c_4$ occur for different values of $x$, any search for an acceptable broadband single-frequency 180° pulse necessarily compromises between initial deviations and bandwidth. We choose to define as an acceptable broadband pulse one where $\Delta\gamma \leq 0.03\gamma_0$ and $\Delta\theta$ and $\Delta\phi$ (the deviations in $\theta$ and $\phi$, respectively) are less than 3° within the entire effective bandwidth of the pulse. For single-frequency-$\pi$ irradiation sequences, a numerical search gives $\Delta\omega_{\max}=\Delta\omega_{\max}/\bar{\omega} \approx 0.26$ for $\Omega_1=1.22$, $\psi_1=\pi$.

Composite single-frequency pulses for other flip angles can also be easily designed by this method. Changes in $\omega_0$, which determine the on-resonance flip angle, change the relative offsets between the $\{|\alpha m\rangle\}$ and the $\{|\beta m\rangle\}$ manifolds, and thus the weights of the various terms in the expansions of Eq. (3.3). Where $J_0(x)=[(\omega-\omega_0)/\omega_0]J_1(x)$ we have a first approximation to $c_2=0$. Smaller values of $x$ are required to minimize deviations in $s_1$ and to achieve greater bandwidths $\Delta\omega_{\max}$. Plots of the zero crossings of $c_2$ and $c_4$, and minimal values of $s_1$, for single-frequency irradiation schemes are given in Fig. 6 as a function of $a_0=\omega_0/\omega$. In each case it appears that $\Omega_1=a_1\omega$ varies linearly with $\omega_0$. A simultaneous solution $c_2=c_4=s_1$ seems possible only for $\omega_0=0$ (although precisely at $\omega_0=0$ the nondegenerate perturbation theory applied in this paper must be replaced by degenerate perturbation theory).

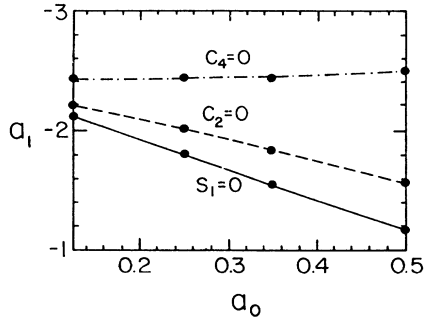


FIG. 6. Calculated values $a_1$ (heavy dots) of single-frequency pulses with different values $a_0$ for the cases $s_1=0$ (——), $c_2=0$ (— — —), and $c_4=0$ (—·—·—·). No intersections occur between these lines in the range of the calculated values of $a_0$ and $a_1$, demonstrating that for finite single-frequency pulses, the parameters $c_2$, $c_4$, and $s_1$ cannot simultaneously be made equal to zero. The on-resonance flip angle is $2a_0\pi$.

### C. Multifrequency modulation schemes

A broadband pulse is one where the terms $c_m(\Delta\omega)^m$ contribute little to the value of $\lambda_n$, and $s_1$ (and all higher-order terms $s_m$, however they might be defined) is small. The simplest solution, which is infinitely broadband, is $c_2=c_4=\cdots=c_m=0$, and similarly for all $s_m$. That such a solution exists for achievable values of $\omega_n$ and arbitrary $\omega_0$ is far from clear, although the existence of infinitely broadband inversion pulses[5,25,26] and the phenomenon of self-induced transparency[28] suggest that for certain $\omega_0$ it may be possible. Instead, we work to minimize the effect of the entire series of terms.

For the moment we concentrate on the terms $c_m$. A completely analogous argument holds for the $s_m$. Clearly, if the power-series expansion for $\lambda$ is to diverge only minimally from its on-resonance value for $\Delta\omega\approx 0$, we require $c_2\approx 0$. Somewhat further off resonance, terms in $c_4(\Delta\omega)^4$ become more important. We consider the polynomial expression $c_2(\Delta\omega)^2+c_4(\Delta\omega)^4$. It has an extremum of $-c_2^2/4c_4$ at $\Delta\omega=\sqrt{-c_2/2c_4}$ and, if $c_2$ and $c_4$ are of opposite sign, a zero crossing at $\Delta\omega=\sqrt{-c_2/c_4}$. In order to extend the range of $\Delta\omega$ for which this polynomial is small, we require that $c_2$ be small, that $c_4$ be of the same magnitude, and that they be of opposite sign. At larger offsets, the $c_6$ and $c_8$ coefficients also become relevant.

As $c_4$ is generally smaller than $c_2$ (because $|\delta_n|<\frac{1}{2}$), an initial approximation to a broadband excitation sequence is identified by finding pulse parameters $\Omega_n$ which minimize the value of $|c_2|$. This condition can generally be achieved for any $\omega_0$ at only a small number of values of $\Omega_m$. We have discussed the general characteristics of single-frequency irradiation schemes above. For single-frequency modulation sequences, it seems impossible to simultaneously satisfy $c_2=c_4=0$, where $0<\omega_0\tau<2\pi$. Some compromise between the initial deviation in $\lambda_n$ and the bandwidth $\Delta\omega_{\max}$ must be struck. Notable improvement in simultaneously minimizing both $c_2$ and $c_4$ can be made by introducing several nonzero $\omega_n$. The surfaces of $c_2\{\omega_n^x\}$ and $c_4\{\omega_n^x\}$ can be easily evaluated numerically, and simultaneous zero crossings identified. As more fields are added, it becomes possible to rigorously minimize $s_1$.

Where it is possible to simultaneously satisfy the pair of conditions $c_2=0$ and $s_1=0$, these $\omega_n$ would result in a broadband-irradiation sequence for some range of $\Delta\omega>0$. Most broadband pulses will have $\{\omega_n\}$ chosen such that the low-order coefficients are small yet not precisely zero, so as to provide some compensation for the finite values of higher-order terms which cause performance to deteriorate at large offsets. Optimization of performance in a broadband sequence generally requires a systematic variation of $\{\omega_n\}$ in some region where the calculated values of $c_2$, $c_4$, and $s_1$ are appropriately small. We can observe that the higher-order corrections are being minimized by counting the number of times $\gamma=\gamma_0$ as a function of $\Delta\omega$, or more accurately by counting the number of zeros in the derivative of $\gamma$ or $\theta$. In principal, we might also calculate these terms by an extension of Eqs. (3.3) and (3.6), but such calculations do not appear practical. For $n_{\max}$ fixed, and thus a finite number of irradiation frequencies $n\omega t$ and amplitudes $\omega_n$, there appears to be a natural maximum bandwidth $\Delta\omega_{\max}$ over which it is possible to achieve uniform excitation. Within that bandwidth, additional constraints (e.g., minimum $\bar{\omega}$ or $\omega_{\max}$) can be imposed, but substantial improvement in the bandwidth $\Delta\omega_{\max}$ seems to require additional irradiation sidebands of significant intensity and not simply more precisely chosen values of the $\Omega_n$. This appears consistent with our understanding that the process we apply leads to minimization of more of the $c_m$ and $s_m$ coefficients at each step. Broad bandwidths also appear to be more difficult to achieve near the extreme values of $\gamma$ (i.e., for $\gamma\leq 45°$ or $\gamma\geq 315°$) than at intermediate rotation angles.

Our procedure for finding broadband pulses is then as follows. First, two or three values of $\Omega_n$ are chosen nonzero (generally, $\Omega_1$, $\Omega_2$, and $\Omega_3$). The expressions for $\delta_n$, $c_2$, $c_4$, and $s_1$ are then evaluated [Eqs. (A9), (3.3), and (3.6)] and simultaneous zero-crossings or near-zero-crossings of the latter three are identified. Starting with these values for the low-order $\Omega_n$ a subsequent search is performed which investigates the propagator $U(0,\tau,\Delta\omega)$ itself, in order to maximize the bandwidth of uniform excitation. In the final search, additional nonzero $\Omega_n$ were introduced, occasionally including $\Omega_4$. The ultimate criterion for uniform excitation is necessarily an arbitrary one. One measure which has been suggested is deviations in the quaternion. We have chosen instead to define a bandwidth given by $\Delta\omega_0$ within which the rotation angle $\gamma$ deviates by no more than 3% from its on-resonance ideal value, and that neither the polar angles $\theta$ or $\phi$ deviate by more than 3°. So as to identify the bandwidth independent of the rather trivial observation that doubling the applied field also doubles the absolute bandwidth, we define the range of satisfactory excitation via the dimensionless parameter $\Delta\omega_{\max}$. While there appears to be a whole set of families of solutions which would satisfy our criterion as broadband-excitation sequences, we focused on those solutions which were found for the lowest values of $\bar{\omega}$. For any desired rotation angle $\gamma$ the uniform excitation bandwidth is maximized for a fixed number of nonzero $\Omega_n$. If the bandwidth thus achieved is insufficient, then additional sidebands might be introduced.

### D. Calculations

The numerical calculation of the $\delta_n$ values from the $\Omega_n$ and $\psi_n$ parameters of the irradiation field was accomplished in either of two fashions. In the first case, the $\delta_n$ are calculated by numerical diagonalization of the matrix $\omega N+\sum_n \omega_n Z_n$. The submatrix of $\omega N+\sum_n \omega_n Z_n$ in the $|\alpha k\rangle, |\alpha k\rangle$ manifold of states was generated for a finite number of $\pm k$ values only. The dimension $k$ of the truncated square matrix was chosen by checking for convergence of the eigenvector elements. In most cases $k=30$ proved sufficient. The diagonalization of this matrix results in a truncated representation of the matrix $\underline{d}$ [see

Eqs. (2.38) and (B1)]. Given $\underline{d}$, the elements $\delta_n$ are obtained using Eq. (A3). The $\delta_n$ values might also be calculated directly using the prescription of Appendix A, where they are expressed in terms of the Bessel functions $J_p(\Omega_k/k\omega)$. A finite number of Bessel functions $J_p$ were calculated so as to truncate the otherwise infinite sum in this equation. Only Bessel functions $J_p(\Omega_k/k\omega) > 5 \times 10^{-5}$ were included in the summations. For fields of moderate strengths, no more than the first eight Bessel functions ($J_0 - J_7$) were required.

Given the $\{\delta_n\}$, $c_2$, $c_4$, and $s_1$ were evaluated using Eqs. (3.3b), (3.3c), and (3.6), respectively. Sets of $\Omega_n$ values for which both $c_2 \approx 0$ and $s_1 \approx 0$ were found by varying the $\Omega_n$ while checking for values at which both conditions were simultaneously satisfied. These calculations were done on an IBM-320 computer and, occasionally, on an IBM PC-AT microcomputer. The evaluation of the evolution operator elements was performed on a PC-AT. The time-dependent Hamiltonian $\mathcal{H}(t)$ was approximated by a large number of piecewise time-independent steps at the average value of $\mathcal{H}(t)$ during the appropriate interval. The propagator for that interval was calculated and appended to the product of all previous intervals. The process was repeated until further subdivision gave no significant change in the final result. When the number of steps was at least 100 times the largest frequency component, convergence was good. Given $U(0,\tau)$ the pulse parameters $\gamma(\Delta\omega)$, $\theta(\Delta\omega)$, and $\phi(\Delta\omega)$ could be derived from Eqs. (2.29). Optimization of pulse shapes was achieved by taking the sum of the mean-square deviations between the propagators calculated for $\Delta\omega = 0$ and some set of offsets up to a threshold offset. The final stage of optimization involved human intervention to choose between closely related solutions.

### E. Broadband excitation pulses: Results

Because the number of possible Fourier coefficients $\Omega_n$ and phases $\psi_n$ in Eq. (2.4) can easily become large, we restricted ourselves, as we explained previously, to broadband-excitation pulses where $\psi_n = 0$ or $\pi$. With this restriction an amplitude-modulated-irradiation sequence of length $\tau$ can be defined uniquely by a set of Fourier coefficients

$$a_n = \pm \frac{\Omega_n}{\omega} , \tag{3.9}$$

where the $\pm$ sign corresponds to $\psi_n = 0, \pi$. With this condition the pulses become symmetric in time with respect to their centers, and therefore the pulse-response parameter $\phi = 0$ independent of $\Delta\omega$. The value $a_0$ equals the on-resonance effective pulse strength, and the $a_n$ values together define the shape of the irradiation. For $\tau = 1$, a $\gamma_0 = 90°$ pulse corresponds to $a_0 = \frac{1}{4}$. In the same way, 45°, 135°, or 180° correspond to $a_0 = \frac{1}{8}$, $\frac{3}{8}$, and $\frac{1}{2}$, respectively.

Following the search procedure described above, $a_n$ values are found which satisfy the two conditions $c_2 = s_1 = 0$. Four irradiation sequences are considered in this paper, namely, broadband 45°, 90°, 135°, and 180° pulses. The choice of these particular flip angles was, from a theoretical perspective, arbitrary, although from an experimental perspective this set includes several of the most useful flip angles in coherent spectroscopy. We wish to emphasize that there exists a continuum of solutions for all possible flip angles. The preliminary search was carried out for only three nonzero Fourier coefficients $a_1$, $a_2$, and $a_3$. The range of values investigated was $-3 \le a_1 \le 3$, $-3 \le a_2 \le 3$, and $-4 \le a_2 \le 4$. Paths in the three-dimensional parameter space described by $a_1$, $a_2$, and $a_3$, where both $c_2$ and $s_1$ are zero, are calculated and presented in Tables I–IV.

TABLE I. Coefficients $a_n$ describing a portion of the path where $c_2 = s_1 = 0$ and $c_4$ is small for only $\{a_1, a_2, a_3 \neq 0\}$ and $a_0 = 0.125$ (i.e., a $\pi/4$ pulse). Listed are all of the nonzero $a_n$, the rms field $\bar{\omega}$, and the calculated value of $c_4$. The amplitudes of the modulation sidebands are restricted to fall in the range $-3 \le a_1 \le 3$, $-3 \le a_2 \le 3$, and $-4 \le a_2 \le 4$.

| $a_0$ | $a_1$ | $a_2$ | $a_3$ | $\bar{\omega}$ | $c_4$ |
|---|---|---|---|---|---|
| 0.125 | −1.69 | 0.38 | −4.00 | 3.08 | 0.002 |
| 0.125 | −1.75 | 0.36 | −3.50 | 2.78 | −0.009 |
| 0.125 | −1.81 | 0.36 | −3.00 | 2.49 | −0.022 |
| 0.125 | −1.85 | 0.34 | −2.50 | 2.21 | −0.044 |
| 0.125 | −1.90 | 0.34 | −2.00 | 1.97 | −0.062 |
| 0.125 | −1.95 | 0.33 | −1.50 | 1.76 | −0.081 |
| 0.125 | −2.00 | 0.32 | −1.00 | 1.60 | −0.094 |
| 0.125 | −2.05 | 0.31 | −0.50 | 1.51 | −0.106 |
| 0.125 | −2.11 | 0.30 | 0.00 | 1.51 | −0.100 |
| 0.125 | −2.18 | 0.28 | 0.50 | 1.60 | −0.087 |
| 0.125 | −2.26 | 0.27 | 1.00 | 1.76 | −0.069 |
| 0.125 | −2.36 | 0.23 | 1.50 | 1.99 | −0.051 |
| 0.125 | −2.49 | 0.15 | 2.00 | 2.26 | −0.031 |
| 0.125 | −2.71 | 0.05 | 2.50 | 3.15 | −0.012 |

TABLE II. Coefficients $a_n$ describing a portion of the path where $c_2 = s_1 = 0$ and $c_4$ is small for only $\{a_1, a_2, a_3 \neq 0\}$ and $a_0 = 0.25$ (i.e., a $\pi/2$ pulse). Listed are all of the nonzero $a_n$, the rms field $\bar{\omega}$, and the calculated value of $c_4$. The amplitudes of the modulation sidebands are restricted to fall in the range $-3 \le a_1 \le 3$, $-3 \le a_2 \le 3$, and $-4 \le a_2 \le 4$.

| $a_0$ | $a_1$ | $a_2$ | $a_3$ | $\bar{\omega}$ | $c_4$ |
|---|---|---|---|---|---|
| 0.25 | −1.38 | 0.84 | −4.00 | 3.06 | 0.011 |
| 0.25 | −1.44 | 0.79 | −3.50 | 2.75 | 0.003 |
| 0.25 | −1.50 | 0.77 | −3.00 | 2.45 | −0.009 |
| 0.25 | −1.55 | 0.75 | −2.50 | 2.16 | −0.027 |
| 0.25 | −1.61 | 0.72 | −2.00 | 1.90 | −0.046 |
| 0.25 | −1.65 | 0.71 | −1.50 | 1.68 | −0.069 |
| 0.25 | −1.70 | 0.70 | −1.00 | 1.50 | −0.087 |
| 0.25 | −1.76 | 0.67 | −0.50 | 1.40 | −0.100 |
| 0.25 | −1.82 | 0.66 | 0.00 | 1.39 | −0.100 |
| 0.25 | −1.88 | 0.64 | 0.50 | 1.47 | −0.094 |
| 0.25 | −1.95 | 0.60 | 1.00 | 1.62 | −0.081 |
| 0.25 | −2.04 | 0.59 | 1.50 | 1.85 | −0.062 |
| 0.25 | −2.16 | 0.55 | 2.00 | 2.13 | −0.041 |
| 0.25 | −2.33 | 0.43 | 2.50 | 2.49 | −0.022 |
| 0.25 | −2.65 | 0.15 | 3.00 | 2.84 | 0.005 |

TABLE III. Coefficients $a_n$ describing a portion of the path where $c_2=s_1=0$ and $c_4$ is small for only $\{a_1,a_2,a_3\neq 0\}$ and $a_0=0.375$ (i.e., a $3\pi/4$ pulse). Listed are all of the nonzero $a_n$, the rms field $\bar{\omega}$, and the calculated value of $c_4$. The amplitudes of the modulation sidebands are restricted to fall in the range $-3\leq a_1\leq 3$, $-3\leq a_2\leq 3$, and $-4\leq a_2\leq 4$.

| $a_0$ | $a_1$ | $a_2$ | $a_3$ | $\bar{\omega}$ | $c_4$ |
|---|---|---|---|---|---|
| 0.375 | −1.06 | 1.33 | −4.00 | 3.10 | 0.017 |
| 0.375 | −1.13 | 1.26 | −3.50 | 2.78 | 0.015 |
| 0.375 | −1.20 | 1.21 | −3.00 | 2.47 | 0.007 |
| 0.375 | −1.25 | 1.18 | −2.50 | 2.18 | −0.007 |
| 0.375 | −1.30 | 1.15 | −2.00 | 1.91 | −0.027 |
| 0.375 | −1.35 | 1.12 | −1.50 | 1.68 | −0.048 |
| 0.375 | −1.40 | 1.09 | −1.00 | 1.49 | −0.069 |
| 0.375 | −1.46 | 1.08 | −0.50 | 1.38 | −0.081 |
| 0.375 | −1.51 | 1.07 | 0.00 | 1.36 | −0.094 |
| 0.375 | −1.57 | 1.04 | 0.50 | 1.43 | −0.094 |
| 0.375 | −1.64 | 1.02 | 1.00 | 1.58 | −0.087 |
| 0.375 | −1.73 | 0.98 | 1.50 | 1.80 | −0.069 |
| 0.375 | −1.82 | 0.95 | 2.00 | 2.06 | −0.052 |
| 0.375 | −1.96 | 0.90 | 2.50 | 2.37 | −0.031 |
| 0.375 | −2.18 | 0.76 | 3.00 | 2.70 | −0.013 |

Within this limited range, one dominant pathway was found for each choice of $\gamma$. Additional pathways near extreme values in one or several of the parameters, and thus with larger values of $\bar{\omega}$, were also detected. These are not presented here, but will be discussed in a later publication, where many of these pathways and their corresponding pulse characteristics will be summarized.

Given these initial results, there were a number of possible means of proceeding. We have chosen two paths: first, we attempted to find maximal bandwidth-irradiation schemes (which involved addition of a fourth coefficient $a_4$) where the quantity $\overline{\Delta\omega_{\max}}$ was the only measure of quality. Our second effort was to find low-power (with respect to average field $\bar{\omega}$ and peak field $\omega_{\max}$) compensated pulses. Both types of pulses were found for each of the representative rotation angles discussed above. In either case, the irradiation sequences presented are the result of a final search carried out for values of $\{a_i\}$ in the vicinity of the pathways found above.

TABLE IV. Coefficients $a_n$ describing a portion of the path where $c_2=s_1=0$ and $c_4$ is small for only $\{a_1,a_2,a_3\neq 0\}$ and $a_0=0.50$ (i.e., a $\pi$ pulse). Listed are all of the nonzero $a_n$, the rms field $\bar{\omega}$, and the calculated value of $c_4$. The amplitudes of the modulation sidebands are restricted to fall in the range $-3\leq a_1\leq 3$, $-3\leq a_2\leq 3$, and $-4\leq a_2\leq 4$.

| $a_0$ | $a_1$ | $a_2$ | $a_3$ | $\bar{\omega}$ | $c_4$ |
|---|---|---|---|---|---|
| 0.50 | −0.74 | 1.88 | −4.00 | 3.21 | 0.019 |
| 0.50 | −0.81 | 1.74 | −3.50 | 2.87 | 0.020 |
| 0.50 | −0.88 | 1.69 | −3.00 | 2.56 | 0.017 |
| 0.50 | −0.94 | 1.62 | −2.50 | 2.27 | 0.007 |
| 0.50 | −1.00 | 1.57 | −2.00 | 2.00 | −0.009 |
| 0.50 | −1.05 | 1.54 | −1.50 | 1.76 | −0.029 |
| 0.50 | −1.10 | 1.53 | −1.00 | 1.59 | −0.047 |
| 0.50 | −1.15 | 1.51 | −0.50 | 1.48 | −0.062 |
| 0.50 | −1.21 | 1.49 | 0.00 | 1.45 | −0.081 |
| 0.50 | −1.26 | 1.47 | 0.50 | 1.50 | −0.087 |
| 0.50 | −1.33 | 1.44 | 1.00 | 1.64 | −0.081 |
| 0.50 | −1.41 | 1.43 | 1.50 | 1.84 | −0.069 |
| 0.50 | −1.50 | 1.42 | 2.00 | 2.09 | −0.056 |
| 0.50 | −1.62 | 1.40 | 2.50 | 2.38 | −0.037 |
| 0.50 | −1.79 | 1.36 | 3.00 | 2.70 | −0.019 |

### 1. *Broadest-bandwidth pulses*

The identification of the absolute maxima in bandwidth for any given $a_0$ and number of $a_n$ is a fairly difficult procedure and depends strongly on the actual test for quality applied. It is, however, quite generally true that optimal bandwidth pulses are most sensitive to the amplitudes of the lowest-order coefficients $a_n$. A general scheme, useful for predicting the optimal low-order coefficients, has been presented elsewhere.[14(c)] Starting from the coefficients $\{a_1,a_2,a_3\}$ provided by Tables I–IV where $c_2=c_4=s_1=0$, we added an additional sideband with amplitude $a_4$ at frequency $4\omega$, and maximized the bandwidth. This always decreases the optimal value of $|a_2|$. In Table V we provide the coefficients $\{a_n; n=0,\ldots,4\}$ for our broadest bandwidth pulses in the amplitude region we have explored.

It is not clear that there exists any good experimental justification in attempting to improve marginally these results, because it seems unlikely that there exists an experimental apparatus capable of reproducing the pulse shapes to the precision we provide. While the optimum bandwidth is quite sensitive to the precision of the coefficients, at offsets $\Delta\omega$ well within the specified band-

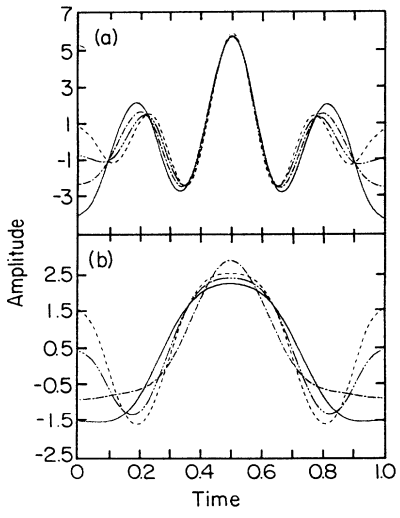


FIG. 7. Time dependence of the pulses defined in Tables V and VI. Solid lines (——) represent the 45° pulses, dash-dotted lines (—·—·—·) represent the 90° pulses, dash-double-dotted lines (—··—) the 135° pulses, and dashed lines (— — —) the 180° pulses. (a) The four-frequency broadest-bandwidth pulses of Table V. (b) The three-frequency low-power pulses of Table VI. Note that the vertical scale is $\frac{1}{2}$ that of (a).

TABLE V. Coefficients $a_n$, the bandwidth $\overline{\Delta\omega_{max}}$, rms field $\bar{\omega}$, and peak field $\omega_{max}$, for optical bandwidth pulses with four modulation sidebands.

| $\gamma$ | $a_0$ | $a_1$ | $a_2$ | $a_3$ | $a_4$ | $\overline{\Delta\omega_{max}}$ | $\bar{\omega}$ | $\omega_{max}$ |
|---|---|---|---|---|---|---|---|---|
| 45° | 0.125 | −1.753 | 0.26 | −3.23 | 0.51 | 0.63 | 2.65 | 5.878 |
| 90° | 0.25 | −1.50 | 0.54 | −2.58 | 1.00 | 0.88 | 2.27 | 5.87 |
| 135° | 0.375 | −1.25 | 0.795 | −2.06 | 1.46 | 1.03 | 2.10 | 5.94 |
| 180° | 0.50 | −1.00 | 1.05 | −1.625 | 1.92 | 1.06 | 2.11 | 6.095 |

width the performance is relatively insensitive to small variations in the specified amplitudes. In situations where the performance at large offsets is critical, it will generally prove more satisfactory to design a broader-bandwidth-irradiation sequence, which appears to be possible by adding further modulation sidebands and additional nonzero $a_n$, rather than to rely upon experimental reproduction of the theoretical performance.[14]

Comparing the broadband-excitation pulses we first see that the required mean pulse intensities decrease for increasing pulse length, while $\overline{\Delta\omega_{max}}$ simultaneously increases. This confirms our observation from single-frequency modulation studies that it is easier to create a 180° pulse than a 45° pulse and that the broadest bandwidths at the lowest values of $\bar{\omega}$ will generally be found for $\omega_0 \approx 0.5$. Our experience with pulse optimization suggests that it is the introduction of additional frequency components which allows us to successively decrease the size of additional terms in the expansion of Eq. (3.3), and that there is a natural bandwidth limitation for any given choice of number of modulation sidebands. Whether the bandwidth limitation can be overcome by choosing to explore the higher-amplitude pathways which we have discovered remains to be explored.

Figure 7(a) presents the time profile of these pulses. These maximum-bandwidth pulses all have similar temporal profiles. At the beginning and end of the cycle the amplitude of the applied field is significantly weaker than it is at the middle of the cycle. This behavior seems characteristic of many composite pulse schemes, where if we observe the trajectories traversed by a representative magnetization vector during the application of the composite pulse most of the evolution generally takes place in the middle of the pulse sequence. Thus the peak power demands can be much greater than the mean.

### 2. *Low-power composite pulses*

In many experimental situations, optimizing the effective excitation bandwidth may not be the most important parameter. Instead, power limitations may make it important to minimize either the average or peak irradiation field without sacrificing too much of the bandwidth.

It is easy, instead, to derive "low-power" pulses using the same basic procedure described above. Given the paths which identify the simultaneous zero crossings of $c_2$ and $s_1$, we chose points where the power requirements as represented by $\bar{\omega}$ were low. Pulses were then optimized for maximum bandwidth $\overline{\Delta\omega_{max}}$ subject to the constraint that $\bar{\omega}$ should remain small. These low-power pulses also seem to have relatively more modest peak power requirements, and should be useful in experimental situations where the average power may not be as great a concern as the limitations imposed by the finite output powers of available amplifiers. The coefficients describing our low-power pulses, and a pictorial representation of these pulses, are given in Tables VI and Fig. 7(b), respectively. By comparison with the broadest-bandwidth pulses presented above, the mean and peak fields are substantially reduced, as is the effective bandwidth.

### 3. *Magnetization pathways*

At all other points in this paper we have referred only to the propagator $U(0,\tau)$, and thus implicitly concerned ourselves with only the net evolution from initial to final states. That the actual evolution of the two-level system under $\mathcal{H}$ is a complicated function of the offsets and the irradiation sequence is illustrated in Figs. 8 and 9, where we provide representative trajectories for the broadest-bandwidth sequences (Fig. 8) and low-power sequences for $\gamma_0 = \pi/2$. For each sequence we have also provided two different initial and final states, both for longitudinal magnetization initially aligned parallel to the $z$ axis [Figs. 8(a) and 9(a)], and for transverse magnetization initially aligned parallel to the $x$ axis. We also provide the trajectories for two offsets within the effective bandwidth $\overline{\Delta\omega} < \overline{\Delta\omega_{max}}$. In all eight cases, a high degree of compensation for the deleterious effects of resonance offset is exhibited.

TABLE VI. Coefficients $a_n$, the bandwidth $\overline{\Delta\omega_{max}}$, rms field $\bar{\omega}$, and peak field $\omega_{max}$, for low-power pulses with three modulation sidebands.

| $\gamma$ | $a_0$ | $a_1$ | $a_2$ | $a_3$ | $\overline{\Delta\omega_{max}}$ | $\bar{\omega}$ | $\omega_{max}$ |
|---|---|---|---|---|---|---|---|
| 45° | 0.125 | −2.1 | 0.2 | 0.2 | 0.30 | 1.50 | 2.225 |
| 90° | 0.25 | −1.7 | 0.7 | −0.2 | 0.50 | 1.33 | 2.85 |
| 135° | 0.375 | −1.5 | 1.0 | 0.5 | 0.50 | 1.38 | 2.375 |
| 180° | 0.50 | −1.2 | 1.5 | 0.7 | 0.50 | 1.53 | 2.50 |

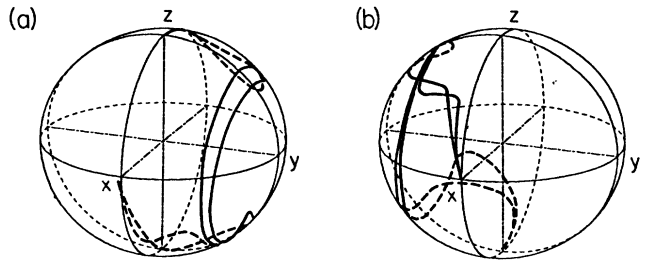


FIG. 8. Calculated trajectories showing the evolution of the tip of the magnetization vector during the four-frequency broadest-bandwidth 90° pulse whose coefficients $\{a_1,a_2,a_3,a_4\}$ are given in Table V. The initial orientation of the magnetization vector is chosen to be parallel to (a) the $z$ axis, and (b) the $x$ axis. For these representations, the pulses are applied in the $y$ direction. Evolution during the pulse is plotted for two resonance offsets: $\overline{\Delta\omega}=0.4$ and $\Delta\omega=0.7$.

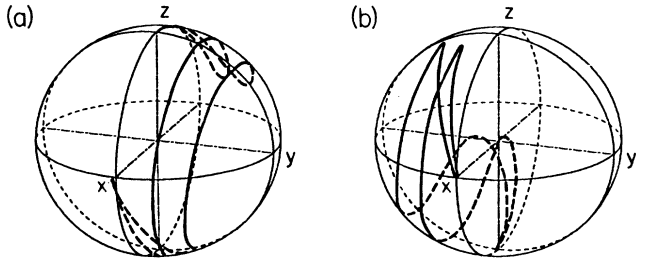


FIG. 9. Calculated trajectories showing the evolution of the tip of the magnetization vector during the three-frequency low-power 90° pulse whose coefficients $\{a_1a_2,a_3\}$ are given in Table VI. The initial orientation of the magnetization vector is chosen to be parallel to (a) the $z$ axis, and (b) the $x$ axis. For these representations, the pulses are applied in the $y$ direction. Evolution during the pulse is plotted for two resonance offsets: $\overline{\Delta\omega}=0.2$ and $\Delta\omega=0.4$.

## IV. CONCLUSIONS

In this paper we have presented a general scheme useful for the analysis of arbitrary irradiation schemes on a two-level system. While we express the irradiation field as a Fourier series, the subsequent transformation between the time-dependent Hamiltonian $\mathcal{H}(t)$ and $H_F$ retains all the essential details of the problem (unlike the linear-response theory). This transformation creates a new problem. Where previously the time dependence of $\mathcal{H}$ made a prediction of the properties of $U(0,\tau)$ difficult, we now encounter the difficulty of diagonalizing an infinite-dimension matrix. The methods of achieving this diagonalization (or approximate diagonalization) depend on the details of the particular problem. For the case we have treated in this paper—broadband, offset-independent-irradiation schemes on two-level systems—we have shown how perturbation theory leads to expressions which provide significant guidance as to appropriate initial values for subsequent numerical optimization. The broadband amplitude-modulated pulses derived from this procedure provide significantly improved performance over composite pulses which have been derived by other equally general treatments. It appears possible to improve the performance of these pulses to a great extent, although we have not yet analyzed the limits. Furthermore, the treatment we have presented allows for the imposition of further constraints without significantly complicating the analysis.

There remain a number of completely unexplored but closely related problems. Perhaps most trivially one might ask as to whether other pathways with different coefficients $\{a_n\}$ might prove more efficient. This is a problem which can be addressed by the very same techniques described in this paper. More fundamental questions about extensions of the Floquet formalism that we have used here might also be asked. The most direct extensions appear to be in the design of broadband-pulse sequences for three-level systems (e.g., spin-1 nuclei), and to optimized narrow-band rather than broadband excitation. We expect both these and other questions to be fruitful avenues in the near future.

## ACKNOWLEDGMENTS

We would like to acknowledge a series of helpful discussions with Dr. A. J. Vega, and the technical assistance of Mr. D. Abramovich. The Israeli Academy of Sciences provided funding in support of this work.

## APPENDIX A

Using Eq. (2.42), we write

$$\Delta=\prod_{n\,(\neq 0)}(e^{(\omega_n/n\omega)Z_n})e^{-i\pi Y_0/2}Z_0e^{i\pi Y_0/2}\times\prod_{n\,(\neq 0)}(e^{-(\omega_n/n\omega)Z_n})\,. \tag{A1}$$

We use the fact that all $Z_n$ operators commute

$$[Z_n,Z_m]=0\,. \tag{A2}$$

The $\Delta$ matrix then takes on the form

$$\Delta=-\frac{1}{2}\begin{bmatrix}(0) & (\underline{d}^2)\\ (\underline{d}^{-2}) & (0)\end{bmatrix}, \tag{A3}$$

where $\underline{d}$ is the submatrix corresponding to $\prod_{n\neq 0}\exp(\omega_n/n\omega)Z_n$ between the states $|\alpha n\rangle$ and $|\alpha m\rangle$. The $\underline{d}$ matrix is treated more extensively in Appendix B. The $\delta_n$ elements of $\Delta$ can be calculated by evaluation of the elements of $\underline{d}^2$, and

$$\delta_n=-\langle\alpha k|\Delta|\beta n+k\rangle=-\frac{1}{2}\left\langle\alpha k\left|\prod_{m\,(\neq 0)}[e^{-(2\omega_m/m\omega)Z_m}]\right|\alpha n+k\right\rangle\,. \tag{A4}$$

To simplify this expression, we first consider only the elements of $Z_n$ between $|\alpha k\rangle$ and $|\alpha k+n\rangle$, whose values are $\frac{1}{2}$. Further, we realize that the $\omega_n$ coefficients are related because

$$\omega_{-n}=\omega_n^*\,. \tag{A5}$$

The elements of $\underline{d}^2$ can therefore be expressed as

$$\delta_n = \frac{1}{2}\left\langle \alpha k \left| \prod_{m\,(>0)} \exp\left[ \frac{2\omega_m}{m\omega} Z_m - \frac{2\omega_m^*}{m\omega} Z_{-m} \right] \right| \alpha n + k \right\rangle , \tag{A6}$$

where the operators enclosed within the parentheses are all Hermitian.

To proceed, let us first calculate $\delta_n$ is the simplest case, where there is only a single time-dependent irradiation field at frequency $\pm(m\omega t)$ and with amplitudes $\omega_m$ and $\omega_{-m}$. In this case, using the expansion of an exponential operator and the fact that the only nonzero elements of $Z_m$ and $Z_{-m}$ have a value of $\frac{1}{2}$ and connect eigenstates $|\alpha k\rangle$ to $|\alpha k+m\rangle$, we can evaluate the expression for $\delta_n$, and

$$\delta_{pm} = -\tfrac{1}{2} \sum_{\substack{k,p \\ k\,(\geq p)}} \frac{1}{k!} \left[ \frac{\omega_m}{m\omega} \right]^k \frac{(-1)^{k-p}}{(k-p)!} \left[ \frac{\omega_m^*}{m\omega} \right]^{k-p} . \tag{A7a}$$

By changing the index of summation we can write, equivalently,

$$\delta_{pm} = -\tfrac{1}{2} \sum_{\substack{k,p \\ k\,(\geq 0)}} \frac{1}{(k+p)!} \left[ \frac{\omega_m}{m\omega} \right]^{k+p} \frac{(-1)^k}{k!} \left[ \frac{m_m^*}{m\omega} \right]^k . \tag{A7b}$$

Expressing $\omega_m$ in terms of a real coefficient $\frac{1}{2}\Omega_m$ and a phase factor $e^{i\psi_m}$ [viz., Eq. (2.4)],

$$\delta_{pm} = -\tfrac{1}{2} \sum_{\substack{k,p \\ k\,(\geq 0)}} \frac{(-1)^k}{k!(k+p)!} \left[ \frac{\Omega_m}{2m\omega} \right]^{2k+p} e^{ip\psi_m}$$

$$= -\tfrac{1}{2} J_p \left[ \frac{\Omega_m}{m\omega} \right] e^{ip\psi_m} , \tag{A8}$$

where we used the infinite-series definition of the Bessel functions $J_p(x)$.

Finally, the matrix elements of $\Delta$ for an arbitrary irradiation sequence with $n_i$ nonzero $\Omega_m$ can be written as

$$\delta_n = -\tfrac{1}{2} \sum_{\substack{n_2,n_3,\cdots \\ n_1 = n-2n_2-3n_3-\cdots}} J_{n_1}\left[ \frac{\Omega_1}{\omega} \right] J_{n_2}\left[ \frac{\Omega_2}{2\omega} \right] J_{n_3}\left[ \frac{\Omega_3}{3\omega} \right] \cdots e^{[i(n_1\psi_1 + n_2\psi_2 + n_3\psi_3 + \cdots)]} , \tag{A9}$$

where we make use of the fact that all operators of the form $\exp[i(\omega_m/m\omega)Z_m]$ commute.

## APPENDIX B

The matrix $D$ of Eq. (2.38) is composed of four submatrices, which are related by Eq. (2.39). A convenient representation of $D$ is

$$D = \frac{1}{\sqrt{2}} \begin{bmatrix} (\underline{d}) & (\underline{d}) \\ -(\underline{d}^{-1}) & (\underline{d}^{-1}) \end{bmatrix} , \tag{B1}$$

where $\underline{d}$ is a unitary submatrix with elements

$$\langle \alpha n|\underline{d}|\alpha m\rangle = \langle \alpha n+k|\underline{d}|\alpha m+k\rangle . \tag{B2}$$

Thus the sum of all row elements of $\underline{d}$ are equal:

$$\sum_{\mathbf{n}} \langle \alpha 0|\underline{d}|\alpha n\rangle = \sum_{\mathbf{n}} \langle \alpha k|\underline{d}|\alpha n+k\rangle . \tag{B3}$$

The real eigenvalue of any unitary matrix equals 1, and

$$D(\mathbf{1}) = \sum_{\mathbf{n}} \langle \alpha 0|\underline{d}|\alpha n\rangle(\mathbf{1}) , \tag{B4}$$

where $(\mathbf{1})$ is an infinite vector all of whose elements equal 1. The sum of all row and column elements of $\underline{d}$ are therefore equal, and using Eq. (B2),

$$\sum_{\mathbf{n}} \langle \alpha 0|\underline{d}|\alpha n\rangle = \sum_{\mathbf{n}} \langle \alpha n|\underline{d}|\alpha 0\rangle = 1 . \tag{B5}$$

The important consequence of this statement is that Eq. (B5) in conjunction with Eq. (B1), proves

$$\sum_{\mathbf{n}} \langle \alpha n|D|\alpha 0\rangle = \sum_{\mathbf{n}} \langle \alpha n|D|\beta 0\rangle = \frac{1}{\sqrt{2}} . \tag{B6}$$

A similar statement holds for $\underline{d}^{-1}$, and therefore

$$\sum_{\mathbf{n}} -\langle \beta n|D|\alpha 0\rangle = \sum_{\mathbf{n}} \langle \beta n|D|\beta 0\rangle = \frac{1}{\sqrt{2}} . \tag{B7}$$

[1] M. H. Levitt and R. Freeman, J. Magn. Reson. **33**, 473 (1979); R. Freeman, S. P. Kempsell, and M. H. Levitt, *ibid.* **38**, 453 (1980).

[2] M. H. Levitt, Prog. Nucl. Magn. Reson. Spectrosc. **18**, 61 (1986).

[3] R. Tycko, Phys. Rev. Lett. **51**, 775 (1983).

[4] R. Tycko, E. Schneider, and A. Pines, J. Chem. Phys. **81**, 680 (1984).

[5] M. S. Silver, R. I. Joseph, C.-N. Chen, V. J. Sank, and D. I. Hoult, Nature **310**, 681 (1984); M. S. Silver, R. I. Joseph, and D. I. Hoult, Phys. Rev. A **31**, 2753 (1985).

[6] W. S. Warren, J. Chem. Phys. **81**, 5439 (1984); M. A. McCoy and W. S. Warren, J. Magn. Reson. **65**, 178 (1985); F. Loaiza, M. A. McCoy, S. L. Hammes, and W. S. Warren, *ibid.* **77**, 175

(1988).
[7]R. Tycko and A. Pines, J. Magn. Reson. **60**, 156 (1984).
[8]R. P. Feynmann, F. L. Vernon, and R. W. Hellworth, J. Appl. Phys. **28**, 49 (1957).
[9]J. S. Waugh, J. Magn. Reson. **50**, 30 (1982).
[10]M. H. Levitt, R. Freeman, and T. Frenkiel, Adv. Magn. Reson. **11**, 47 (1982); A. J. Shaka and J. Keeler, Prog. Nucl. Magn. Reson. Spectrosc. **19**, 47 (1987).
[11]A. J. Shaka and A. Pines, J. Magn. Reson. **71**, 493 (1987).
[12]J. Baum, R. Tycko, and A. Pines, J. Chem. Phys. **79**, 4643 (1983).
[13]J. W. Carlson, J. Magn. Reson. **67**, 551 (1986); J. Mao, T. H. Mareci, K. N. Scott, and E. R. Andrew, *ibid.* **70**, 310 (1986); J. B. Murdoch, A. H. Lent, and M. R. Kritzer, *ibid.* **74**, 226 (1987).
[14](a) D. B. Zax, G. Goelman, and S. Vega, J. Magn. Reson. **80**, 375 (1988); (b) G. Goelman, S. Vega, and D. B. Zax, *ibid.* **81**, 423 (1989); (c) D. B. Zax and S. Vega, Phys. Rev. Lett. (to be published).
[15]A. G. Redfield, S. D. Kunz, and E. K. Ralph, J. Magn. Reson. **19**, 114 (1975).
[16]P. J. Hore, J. Magn. Reson. **54**, 239 (1983); **55**, 283 (1983).
[17]D. L. Turner, J. Magn. Reson. **54**, 146 (1983).
[18]G. A. Morris and R. Freeman, J. Magn. Reson. **50**, 316 (1982).
[19]M. H. Levitt, R. Freeman, and T. Frenkiel, J. Magn. Reson. **47**, 328 (1982).
[20]A. J. Shaka, J. Keeler, T. Frenkiel, and R. Freeman, J. Magn. Reson. **52**, 335 (1983); A. J. Shaka, J. Keeler, and R. Freeman, *ibid.* **53**, 313 (1983).
[21]J. R. Garbow, D. P. Weitekamp, and A. Pines, Chem. Phys. Lett. **93**, 504 (1982).
[22]M. H. Levitt, D. Suter, and R. R. Ernst, J. Chem. Phys. **80**, 3064 (1984).
[23]R. Tycko, E. Schneider, and A. Pines, J. Chem. Phys. **81**, 680 (1984).
[24]T. M. Barbara, R. Tycko, and D. P. Weitekamp, J. Magn. Reson. **62**, 54 (1985); S. Wimperis and G. Bodenhausen, Chem. Phys. Lett. **132**, 194 (1986).
[25]J. Baum, R. Tycko, and A. Pines, Phys. Rev. A **32**, 3435 (1985).
[26]L. Allen and J. H. Eberly, *Optical Resonance and Two-Level Atoms* (Wiley, New York, 1975).
[27]U. Haeberlen and J. S. Waugh, Phys. Rev. **175**, 453 (1968); U. Haeberlen, Adv. Magn. Reson. Supp. I (1976).
[28]S. L. McCall and E. L. Hahn, Phys. Rev. **183**, 457 (1969).
[29]W. Magnus, Commun. Pure Appl. Math. **7**, 649 (1954); P. Pechukas and J. C. Light, J. Chem. Phys. **44**, 3897 (1966); R. M. Wilcox, J. Math. Phys. **8**, 962 (1967); I. Bialynicka-Birula, B. Mielnik, and J. Plebanski, Ann. Phys. (Paris) **51**, 187 (1969).
[30]M. M. Maricq, Phys. Rev. B **25**, 6622 (1982).
[31]J. H. Shirley, Ph.D. thesis, California Institute of Technology, 1963 (unpublished); Phys. Rev. **138B**, 979 (1965).
[32]E. M. Krauss and S. Vega, Phys. Rev. A **34**, 333 (1986); G. Goelman, D. B. Zax, and S. Vega, J. Chem. Phys. **87**, 31 (1987).
[33]S. Vega, E. T. Olejniczak, and R. G. Griffin, J. Chem. Phys. **80**, 4832 (1984); A. Schmidt, S. O. Smith, D. P. Raleigh, J. E.Roberts, R. G. Griffin, and S. Vega, *ibid.* **85**, 4284 (1986); A. Schmidt and S. Vega, *ibid.* **87**, 6895 (1987).
[34]Y. Zur, M. H. Levitt, and S. Vega, J. Chem. Phys. **78**, 5293 (1983).
[35]A. J. Shaka, Chem. Phys. Lett. **120**, 201 (1985).
[36]R. Tycko, A. Pines, and J. Guckenheimer, J. Chem. Phys. **83**, 2775 (1985).
[37]A. Dalgarno, in *Quantum Theory,* edited by D. R. Bates (Academic, New York, 1961), Vol. I, Chap. 5; J. O. Hirschfelder, W. Byers Brown, and S. T. Epstein, Adv. Quantum Chem. **1**, 255 (1964).
[38]C. P. Slichter, *Principles of Magnetic Resonance,* Vol. 1 of *Springer Series in Solid State Sciences* (Springer, New York, 1978), Appendix D.